UNCLASSIFIED

SECURITY CLASSIFICATION OF THIS PAGE

(2)

REPORT DOCUMENTATION PAGE

Form Approved
OMB No. 0704-0188

1a. REPORT SECURITY CLASSIFICATION Unclassified	1b. RESTRICTIVE MARKINGS
2a. SECURITY CLASSIFICATION AUTHORITY	3. DISTRIBUTION/AVAILABILITY OF REPORT Approved for public release; distribution is unlimited
AD-A234 831	5. MONITORING ORGANIZATION REPORT NUMBER(S) AFOSR-TR-91 0379
6a. NAME OF PERFORMING ORGANIZATION Illinois Inst. of Technology 6b. OFFICE SYMBOL (If applicable)	7a. NAME OF MONITORING ORGANIZATION AFOSR/NA
6c. ADDRESS (City, State, and ZIP Code) Department of Civil Engineering Illinois Institute of Technology Chicago, Illinois 60616	7b. ADDRESS (City, State, and ZIP Code) Bolling AFB Washington, DC 20332-6448
8a. NAME OF FUNDING/SPONSORING ORGANIZATION AFOSR 8b. OFFICE SYMBOL (If applicable) NA	9. PROCUREMENT INSTRUMENT IDENTIFICATION NUMBER AFOSR-89-0171
8c. ADDRESS (City, State, and ZIP Code) Bolling Air Force Base Washington, DC 20332-6448	10. SOURCE OF FUNDING NUMBERS PROGRAM ELEMENT NO. 61102F; PROJECT NO. 2302; TASK NO. C2; WORK UNIT ACCESSION NO.

11. TITLE (Include Security Classification)
THE HYSTERESIS AND INCREMENTAL COLLAPSE OF COMPLEX STRUCTURES: A PARADIGM FOR THE FATIGUE FAILURE OF MATERIALS

12. PERSONAL AUTHOR(S)
Guralnick, S.A. and Erber, T.

13a. TYPE OF REPORT	13b. TIME COVERED	14. DATE OF REPORT (Year, Month, Day)	15. PAGE COUNT
FINAL	FROM 1/1/88 TO 12/31/90	1991, March	47

16. SUPPLEMENTARY NOTATION

17. COSATI CODES			18. SUBJECT TERMS (Continue on reverse if necessary and identify by block number)
FIELD	GROUP	SUB-GROUP	HYSTERESIS, INCREMENTAL COLLAPSE, FATIGUE FAILURE, FATIGUE DAMAGE

19. ABSTRACT (Continue on reverse if necessary and identify by block number)

The basic objective of this research program is to characterize the development of material fatigue by means of stress-strain hysteresis and acoustic emission measurements. We have conjectured that the accumulation and organization of damage in material fatigue is similar to the progressive failure of structures under cyclic loading. And, specifically, that the endurance limit of a material in fatigue is the analogue of the incremental collapse load of a structure. Since the principal features of the service life and failure of structures can be completely described by hysteresis methods, it is plausible that similar means can be used to characterize the inception and organization of microplastic processes in materials. All of the experimental results obtained during the current research program confirm these conjectures.

20. DISTRIBUTION/AVAILABILITY OF ABSTRACT	21. ABSTRACT SECURITY CLASSIFICATION
☒ UNCLASSIFIED/UNLIMITED ☐ SAME AS RPT. ☐ DTIC USERS	Unclassified
22a. NAME OF RESPONSIBLE INDIVIDUAL Spencer T Wu	22b. TELEPHONE (Include Area Code) (202) 767-6962
	22c. OFFICE SYMBOL AFOSR/NA

DD Form 1473, JUN 86 *Previous editions are obsolete.* SECURITY CLASSIFICATION OF THIS PAGE

UNCLASSIFIED

THE HYSTERESIS AND INCREMENTAL COLLAPSE OF COMPLEX STRUCTURES: A PARADIGM FOR THE FATIGUE FAILURE OF MATERIALS

FINAL REPORT

Submitted to

THE AIR FORCE OFFICE OF SCIENTIFIC RESEARCH

by

The Department of Civil Engineering

of

Illinois Institute of Technology

Chicago

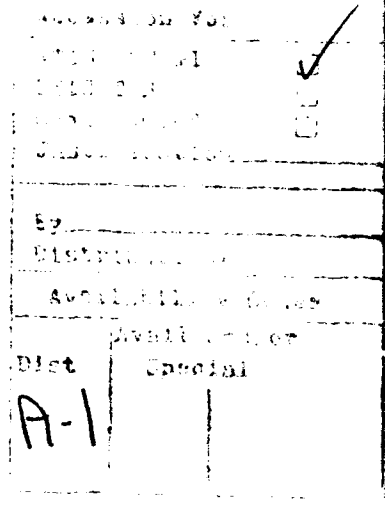

Air Force Grant Number: 2302/B2

Principal Investigator: Dr. S.A. Guralnick

Co-Principal Investigator: Dr. T. Erber

Date of Submission: February 28, 1991

S.A. Guralnick
Principal Investigator

TABLE OF CONTENTS

LIST OF TABLES

LIST OF FIGURES

TECHNICAL ABSTRACT AND SUMMARY

The basic objective of this research program is to characterize the development of material fatigue by means of stress-strain hysteresis and acoustic emission measurements. We have conjectured that the accumulation and organization of damage in material fatigue is similar to the progressive failure of structures under cyclic loading. And, specifically, that the endurance limit of a material in fatigue is the analogue of the incremental collapse load of a structure. Since the principal features of the service life and failure of structures can be completely described by hysteresis methods, it is plausible that similar means can be used to characterize the inception and organization of microplastic processes in materials. All of the experimental results obtained during the current research program confirm these conjectures.

The principal results are the following:

1) Symmetric, strain-controlled loading cycles of unannealed 1018 steel specimens show that the average hysteresis energy dissipated per cycle is a linear function of the strain amplitude.

2) Results from the strain-controlled tests show that average hysteresis energy dissipated per cycle is nearly constant with respect to number of loading cycles while cumulative hysteresis energy dissipated is a function of both strain amplitude and the number of cycles to failure.

3) Uniaxial tension tests show that the proportional limit is approximately equal to the threshold strain ε_{th} for the inception of hysteresis.

4) The correspondence between the shakedown of structures and the endurance limit of materials suggests that the loading threshold for fatigue failure is a phase boundary whose location depends sensitively on plastic microstructure. The general hysteresis theory indicates that this boundary is correlated with the load limit beyond which there is a breakdown of the Kaiser (or, memory) effect in acoustic emission. This trend is confirmed by preliminary experimental results for AE measurements.

1. INTRODUCTION AND BACKGROUND

The failure of structures under repeated loading and the fatigue failure of materials are both important areas of engineering research with extensive literatures. This introduction treats a few essential features that are common to both areas and indicates their relevance to the research effort described herein.

1.1 *Hysteresis, Damage, and Fracture Mechanics*

It is taken for granted that cumulative damage at the microscopic level is the underlying cause for the fatigue of materials. It is also widely believed that the rate at which damage accumulates can be gauged by measuring the areas of stress-strain hysteresis loops -- because it is assumed that these areas correspond to the irreversible hysteresis energy losses that cause damage. However, this chain of argument has been challenged on the practical as well as on the fundamental level: Engineering studies of fatigue going back to the classic work of Foppl [9] and Lazan [10] have demonstrated that there is no straightforward correspondence between the areas of stress-strain hysteresis loops and the onset of fatigue failure. In particular, the comprehensive studies of Morrow [17, 18] and Halford [14, 15] have demonstrated that for a great variety of metals and alloys the cumulative energy input during $\sim 10^6$ cycles to fatigue failure is of the order of 10 times the thermal energy required to bring a sample from room temperature to just above the melting point. Put another way, the energy required to produce fatigue failure in 10^6 loading cycles is 10^4 times the energy needed to produce failure in a single cycle to rupture! These results clearly show that in service conditions leading to fatigue most of the absorbed energy is dissipated harmlessly as heat, and only a small fraction is associated with cumulative damage.

Empirically, it is plausible to identify the damaging component of the energy transfer by a phenomenological parameter, say β; and to estimate the fatigue service life of materials by a suitable adjustment of β. Indeed, the literature contains many attempts of this kind, but success has been elusive. The actual state of affairs is indicated by the fact that designers' handbooks for structural materials such as steels list values of the endurance limit, but omit any mention of damage rates, because there are no reliable measures of β.

There are several fundamental reasons for the failure of this empirical approach.

(a) First, in non-equilibrium situations such as fatigue, the areas of the hysteresis loops do not simply correspond to the rates of energy dissipation. It can be shown quite generally that Warburg's area principle fails in these cases, and that the actual energy losses have to be obtained by non-equilibrium hysteresis methods [11, 12].

(b) Second, the empirical approach utilizes a number of 'state variables' which, in fact, do not exist! This point has been forcefully stated by Bridgman [13]:

> "Classical thermodynamics has had comparatively little to say about irreversible processes and that little has been of a qualitative character, to the effect that during an irreversible process there is an ineradicable increase of the total entropy of the universe. But how much the increase is, or where it is located, is not specified, and in fact the increase of entropy itself has meaning and is defined only if reversible processes exist by which every part of the universe may be brought back from its final to its initial state. But it is safe to say that the majority of actual processes are irreversible, and worse still, most of the objects of daily life such as a plastically strained metal exhibiting hysteresis, are completely surrounded by irreversibility, it being impossible to leave the present state of the body by any path whatever that is not irreversible in detail. The classical entropy concept is thus a concept which is applicable only to a highly idealized set of

conditions and is not applicable in principle, to the commonest situations of daily life."

(c) Third, we have recently extended Bridgman's work on the thermodynamics of plasticity, and obtained the general result that all phenomenological descriptions of damage based on distributed damage coefficients must necessarily conflict with the second law [8]. We show later that this inconsistency points in the direction of a microscopic phenomenology of damage associated with locally fluctuating stress and temperature fields.

The current dominance of fracture mechanics in fatigue research is partially due to the lack of any useful means for assessing the rate of damage accumulation in materials. However, even on the practical level, it is acknowledged that fracture mechanics provides merely an indirect approach to the failure problem --- the existence of significant cracks indicates that the structure has already failed, and fracture mechanics merely sets the limits for the impaired performance of a damaged system, much like the management of a human patient who has already suffered a coronary infarct. The optimum goal of practical design is to match the service conditions with the structure and materials without acc pting any impairment --- and this means unequivocally identifying the true endurance limit and the intrinsic damage absorption capacity of the system.

1.2 *The Shakedown of Structures and the Endurance Limit of Materials*

It is well known that there are loading programs for structures that have beneficial effects --- in practice one says that such structures 'shake down.' This is an important technical illustration of stabilizing hysteresis. However, for every structure and class of loading

programs, there is a critical upper limit of loading beyond which the hysteresis becomes destructive. In these cases the structures fail through the formation of critical sets of plastic hinges that cause incremental collapse [2, 4, 5, 6, 7]. It has been suggested [3] that the shakedown limit of a structure is analogous to the endurance limit of a material. In both situations the systems have effectively infinite service lives when subjected to programs of repeated loading provided that the maximum loads remain below the shakedown and endurance limits in the respective cases.

In the structural situations, the safe load limits are bounded by an incremental collapse envelope [2, 3]: this locus give a unified description of alternating plasticity, plastic collapse, and incremental collapse. It is striking that this failure criterion for structures is analogous to the Goodman-Gerber diagram for the fatigue limits of materials.

There are several other suggestive similarities between incremental collapse and fatigue. For instance, the maximum load range versus the number of cycles to failure for structures yields plots which are completely analogous to the S-N curves for fatigue. Furthermore, the cumulative damage relations for structures are analogous to the Palmgren-Miner [16, 19] laws of fatigue. The significance of these analogies has been discussed in [1, 2, 3, 4, 5, 6, 7].

1.3 *Fatigue: A New Approach Based on the Hysteresis of Complex Systems*

The relation of the structural hysteresis theory to incremental collapse can be summarized as follows:

mechanical work
↓
asymptotic hysteresis above shakedown
↓
formation of incremental collapse mechanisms
↓
accumulation of hinge damage
↓
failure

(A)

We conjecture that a similar sequence is associated with the fatigue failure of materials:

mechanical work
↓
asymptotic hysteresis above the endurance limit
↓
formation of micro-plastic flow patterns
↓
accumulation of lattice imperfections (damage)
↓
threshold of microcrack formation
↓
crack propagation
↓
fracture

(B)

The transition from stabilizing to destructive hysteresis occurs at the shakedown limit in (1) and at the endurance limit in (2). This criterion can be used to locate the critical load in ranges in the respective cases without resorting to the time consuming process of constructing S-N curves. If the loading is sufficiently high so as to overlap the range of destructive hysteresis, then it is generally necessary to obtain estimates of the number of cycles to failure. This intrinsic 'age' of the failure process can also be obtained by hysteresis methods [3, 4, 5, 6, 7].

2. A NEW CONCEPTUAL FRAMEWORK FOR THE PREDICTION OF FATIGUE RESISTANCE

2.1 *Conventional Approach*

The currently-accepted approach [17, 18] for describing fatigue life is to express it in terms of strain amplitude versus the number of cycle N_f to failure (or in the number of strain reversals $2N_f$ to failure). It is argued that the total strain amplitude $\Delta\varepsilon_t/2$ is composed of two parts: an elastic part $\Delta\varepsilon_e/2$ and a plastic part $\Delta\varepsilon_p/2$. Thus the total strain amplitude may be written as:

$$\frac{\Delta\varepsilon_t}{2} = \frac{\Delta\varepsilon_e}{2} + \frac{\Delta\varepsilon_p}{2} \tag{1}$$

The individual terms on the right hand side of Eq. 1 are then assumed to be given by power law relationships, first given in such form by O.H. Basquin [23] as:

$$\frac{\Delta\varepsilon_e E}{2} = \frac{\Delta\sigma}{2} = \sigma_f'(2N_f)^b \tag{2}$$

and,

$$\frac{\Delta\varepsilon_p}{2} = \varepsilon_f'(2N_f)^c \tag{3}$$

It is noted that Eq. 3 is often known as the Manson - Coffin relationship [21, 22].

The parameters appearing in Eqs. 2 and 3 are defined as:

E = Modulus of elasticity

$\frac{\Delta\sigma}{2}$ = stress amplitude

σ_f' = fatigue strength coefficient, defined by the strain intercept at one load reversal ($2N_f = 1$)

N_f = cycles to failure

ε_f' = fatigue ductility coefficient, defined by the strain intercept at one load reversal ($2N_f = 1$)

b, c = are empirically determined exponents from cyclic strain experiments

Combining Eq. 1, 2 and 3 one obtains the usual expression for strain amplitude versus life (reversals to failure) as,

$$\frac{\Delta\varepsilon_t}{2} = \frac{\sigma_f'}{E}(2N_f)^b + \varepsilon_f'(2N_f)^c \qquad (4)$$

The two terms on the right hand side are usually treated separately by utilizing the results from strain controlled cyclic tests performed on samples of the material. The variable appearing in Eqs. 1 and 4 are related to one another as shown in the diagram of Fig. 1.

When a series of measurements are made on stable hysteresis loops at various stain (or stress) levels, then information of the kind shown in Figs. 2 and 3 can be developed. The information given in these two figures can be used to determine: σ_f', b, ε_f' and c. Values for these constants, in turn, may be substituted into Eq. 4 to yield a strain amplitude versus life relationship for the particular material under investigation.

2.2 *Critique of the Conventional Approach*

The approach outlined above, if useful at all, is applicable only in the low cycle ($N_f < 10^4$ cycles) fatigue range as illustrated in Fig. 4.

Manson [22] has proposed a simpler fatigue resistance relationship predicated on the assumption that the exponents b and c in Eq. 4 are more or less universal constants for a wide variety of materials. With the assumption that b = -0.12 and c = -0.6, Manson's equation of "universal slopes" connects the total strain range $\Delta\varepsilon$ and life N_f (number of cycles to failure) as:

$$\Delta\varepsilon = 3.5 \frac{S_u}{E} N_f^{-0.12} + \varepsilon_f^{0.6} N_f^{-.06} \tag{5}$$

in which,

S_u = Ultimate tensile strength

ε_f = true strain at fracture in tension

E = modulus of elasticity

This relationship has a number of drawbacks including the fact that its does not yield an adequate prediction of behavior in the high-cycle range. Or, in other words, it uses an empirical model which pertains primarily to low-cycle fatigue to predict performance over the entire fatigue range including the high-cycle fatigue range.

The most serious drawback of all approaches which utilize low-cycle fatigue models for predicting high-cycle fatigue performance concerns the initiation and growth of cracking. In low-cycle fatigue, cracks initiate relatively early in the life of the material whereas in

high-cycle fatigue cracks initiate relatively late in the life of the material as shown in Fig. 5. Hence, low-cycle fatigue, which is strongly influenced by large plastic deformations, is also influenced by cracking whereas high-cycle fatigue is only weakly influenced by these two factors.

2.3 *Proposed Theory*

The theory proposed herein presupposes that the fatigue process evolves through four stages: (1) the inception of isolated microscopic zones of plasticity, (2) the 'organization' of the microscopic zones of plasticity into macroscopic plastic regions, (3) the initiation of cracks and (4) complete separation or rupture. Stage 1 probably occurs at very low stress levels and if the stresses remain low, fatigue failure does not occur. At higher stress levels, exceeding those needed to initiate microscopic yielding, stage 2 occurs, and this is illustrated by the curve marked P in Fig. 6. If the stresses are raised to still higher levels then stage 3 or crack initiation, occurs as illustrated by the curve marked F in Fig. 6. This curve is sometimes called, "French's line of damage." [20] When the stresses are raised to even higher levels, the cracks which first appeared in state 3 propagate and eventually cause rupture as illustrated by the uppermost curve in Fig. 6. This last curve is the conventional S-N (or Wöhler) curve.

It is clear from Fig. 6 that the entire fatigue process (stage 1 through stage 4) evolves quite differently in the low-cycle region and in the high-cycle region. By carefully monitoring the development of hysteresis, and acoustic emission signals, one can sensitively describe and predict the entire fatigue process both in the low-cycle as well as in the high-cycle region.

The goal of the research effort is to develop a set of diagnostic tests that will permit the prediction of the entire S-N (low cycle and high cycle) curve for a metal from a relatively small number of measurements. A typical S-N curve obtained by conventional means is shown in Fig. 7.

3. RESULTS

3.1 *Materials Properties*

The purpose of this research effort is to investigate the evolution of hysteresis in metals subjected to cyclic stress regimes for the purpose of elucidation of the connection between hysteresis and fatigue strength. To this end, 72 specimens were subjected to axially-applied cyclic stress regimes. Ten specimens of this material were fabricated into ASTM Type 2 axial-load tension specimens, as shown in Fig. A, and stressed to failure. The mechanical properties measured during these 10 tests are given in Table 2. In all cases, the stress-strain diagrams obtained were of the 'gradual yielding' type as shown by the curves labeled 'monotonic' in Figs. 8a and 8b. The average physical properties found were:

Yield Point σ_y	=	70,769 psi
Ultimate Strength, σ_u	=	77,717 psi
Modulus of Elasticity, E	=	29,600,000 psi
Elongation in 2",	=	18.20%
Reduction in Cross - Sectional Area,	=	61.05%

Because the material was of the gradual yielding type, the yield point was measured by the 0.2% offset method using the actual stress-strain curves generated by an X-Y recorder driven by electronic signals emanating from a load cell attached to the testing machine (B-L-H 60,000 lb. UTM) and from a LVDT extensometer attached to the specimen.

Thirteen specimens were fabricated into the shape shown in Fig. B. These 13 specimens were cut to shape by turning a high-speed tracer lathe employing a carbide cutting tool and meticulously hand polished to remove any surface blemishes or cutting

marks visible in a 2X magnifying lens. Each of these 13 specimens was then mounted, in turn, in a MTS servo-value controlled axial load testing machine and subjected to strain-controlled, cyclically-varying tension and compression loads until complete rupture occurred. The speed of testing was 0.1 cycles per second. A sufficient number of stress-strain points were accumulated during each test to obtain the average hysteresis losses per cycle. The corresponding cumulative hysteresis loss information is given in Table 3. Also, this data was used to create the hysteresis loops and the cyclic stress-stain curve shown in Fig. 8a. The latter diagram is merely an empirical curve which is constructed to pass through the tips of the hysteresis loops. This cyclic stress-strain curve is also shown in Fig. 8b in which the hysteresis loops have been removed for greater clarity.

The conventional approach to the treatment of the fatigue behavior of metals has been described in Section 3.1. With the data obtained from the tests performed on the specimens listed in Table 3, it is possible to construct the graphs shown in Figs. 9, 10 and 11, and to find the empirical coefficients defined by Eq. 2, 3 and 4. It was found from these experiments that the data could be 'fitted' by the following three equations which were, respectively, of the form given by Eqs. 2, 3 and 4.

$$\frac{\Delta \varepsilon_e E}{2} = \frac{\Delta \sigma}{2} = \sigma_f'(2N_f)^b = 79.7(2N_f)^{-.05357} \tag{6}$$

$$\frac{\Delta \varepsilon_p}{2} = \varepsilon_f'(2N_f)^c = 0.2034(2N_f)^{-.5081} \tag{7}$$

$$\frac{\Delta \varepsilon_t}{2} = \frac{\sigma_f'}{E}(2N_f)^b + \varepsilon_f'(2N_f)^c$$

or,

$$\frac{\Delta \varepsilon_t}{2} = 79.7\,(2N_f)^{-.05357} + 0.2034\,(2N_f)^{-.5081} \qquad (8)$$

The information given in Tables 1, 2, and 3; Figs. 8a, 8b, 9, 10 and 11; and Eqs. 6, 7 and 8 is believed to be sufficient to fully describe and characterize the mechanical properties of the single batch of material from which all of the test specimens were made.

3.2 *The Evolution of Hysteresis*

The 59 specimens shown in Table 4 were fabricated in the same manner as those shown in Table 3 and subjected to various strain limited, cyclically-applied loading programs in order to investigate the evolution of hysteresis in the low cycle fatigue region (i.e. $N_f < 10^4$). Some of these specimens were subjected only to constant strain range loading, while others were subjected to load regimes which caused the strain amplitudes to vary with the cycle number N in the manner shown in Fig. 12. This type of loading was utilized to obtain as much hysteresis data at various strain amplitudes as possible from a single specimen. This is preferable to collecting data from a number of individual specimens with each specimen subjected only to a single strain amplitude.

Apart from a few cycles at the beginning and a few cycles at the end of the loading history of each specimen, the hysteresis loss (area of the hysteresis loop, ΔU_i) per cycle was found to be very nearly a constant in all cases. This result is typified by the graphs shown in Figs. 13a, b and c. Also, the average hysteresis loss per cycle $< \Delta U_i >$ for every cycle of load to failure is given in the right hand column of Table 4 for all 59 test specimens.

Inasmuch as the hysteresis loss per cycle is very nearly a constant from cycle to cycle during most of the loading history of each specimen, it is clear that the respective cumulative hysteresis loss, $U = \sum_{i=1}^{N} \Delta U_i$, must be very nearly a linear function of N. In other words, this result implies that,

$$\sum_{i=1}^{N} \Delta U_i \cong <\Delta U_i>(N) \tag{9}$$

in which $< \Delta U_i >$ is equal to the average hysteresis loss per cycle; that is, a constant. This result is exemplified by the graphs shown in Figs. 14a and 14b, where it is clear that the $\sum \Delta U_i$ versus N relationship is very nearly a straight line almost up to and including the point of failure. At failure, the total accumulated hysteresis loss is,

$$U_f = \sum_{i=1}^{N_f} \Delta U_i \tag{10}$$

This quantity has been obtained for each of 13 tests. If one makes a graph of U_f versus the number of cycles to failure N_f, as is done in Fig. 15, then it is quite clear that the data is well represented by a straight line on a log-log chart which has the functional form:

$$U_f = c(N_f)^d \tag{11}$$

In this investigation it has been found that fitting the data with an equation of the form of Eq. 11 yields the result,

$$U_f = 26.74\ (N_f)^{1/2}. \tag{12}$$

Although it has been found that hysteresis loss per cycle ΔU_i is very nearly constant with respect to the number of cycles of load application, the average hysteresis loss per cycle $< \Delta U_i >$ is a monotonically increasing function of the strain amplitude $\frac{\Delta \varepsilon_t}{2}$. That is, one may write,

$$< \Delta U_i > = F\left(\frac{\Delta \varepsilon_t}{2}\right) \tag{13}$$

The explicit dependence of $< \Delta U_i >$ upon $\frac{\Delta \varepsilon}{2}$ is shown in Figs. 16a and 16b. It is clear from these two figures that the data may be fitted with three straight lines; the slopes of which increase as the strain amplitude increases.

Although the average hysteresis loss per cycle $< \Delta U_i >$ depends only on the strain amplitude, the cumulative hysteresis loss to failure U_f is a function both of the number of cycles to failure N_f and the strain amplitude $\Delta \varepsilon_t/2$. Formally, this is expressed by,

$$U_f = U_f\left(N_f, \frac{\Delta \varepsilon_t}{2}\right). \tag{14}$$

Eq. 14 implies that the function U_f corresponding to the data given in Table 3, may be used to construct a three dimensional graph of the form shown in Fig. 17. This graph clearly displays the three dimensional trend that as the strain amplitude decreases, the number of cycles to failure increases and the cumulative hysteresis losses also increase.

3.3 *The Connection Between Hysteresis and Fatigue Strength*

The three-dimensional graph shown in Fig. 17 suggests that the connection between U_f, N_f and $\frac{\Delta \varepsilon_t}{2}$ might be exploited to yield further insights into the behavior of materials subjected to cyclic loads. The projection of the space curve shown in Fig. 17 onto the $\frac{\Delta \varepsilon_t}{2}$ - N_f plane gives rise to the plane curve shown in the upper portion of Fig. 18 and the projection of this same space curve onto the U_f - N_f plane gives rise to the plane curve shown in the lower portion of Fig. 18. From both the upper curve as well as the lower curve of Fig. 18, it is clear that the response of the material to cyclically-applied loads when $N_f < 10^4$ differs qualitatively and quantitatively from the response when $N_f > 10^4$. The value $N_f = 10^4$ is, of course, the usual demarcation between low-cycle fatigue and high-cycle fatigue behavior. It is also striking, from the curves of Fig. 18, that the magnitude of the cumulative hysteresis energy dissipated, U_f, grows rapidly as $\frac{\Delta \varepsilon_t}{2}$ decreases and N_f increases. This leads one to the hypothesis that much of the hysteresis energy that is imparted to the material must be dissipated harmlessly as heat while only a relatively small amount of this energy results in actual damage to the material.

4. CONCLUSIONS

The connection between hysteresis and fatigue assumes its simplest form in repetitive strain-controlled loading cycles. Under these circumstances the average hysteresis energy dissipation per cycle is a linear function of the strain amplitude. Since hysteresis is an inherently non-linear and history-dependent process, it is extremely useful to obtain a simple linear relation that governs its behavior. The linear variation of $< \Delta U_i >$ with strain amplitude is consistent with the behavior predicted by the general hysteresis theory, and also strengthens the correspondence between material fatigue and structural failure. On the basis of these results fatigue life N_f, peak strain ε, average hysteresis energy dissipation per cycle $< \Delta U_i >$, and total hysteresis energy dissipation, can all be related by simple power laws.

The hysteresis threshold strain ε_{th} has a dual significance: (1) It may locate the approximate value of the endurance limit, i.e. the loading bound for 'infinite' service life; and (2) it also implies that mechanical hysteresis is a necessary but not a sufficient condition for fatigue failure. A good deal of the confusion in the literature concerning the connection between hysteresis and fatigue can be traced to this gap between 'necessary' and 'sufficient'. The essential distinction is that it is in principle possible to have non-vanishing, steady hysteresis, without any progressive accumulation of damage, or a reordering of the existing damage. The material has, so to speak, sustained an infarct, but can tolerate its effects indefinitely provided that the external loading does not exceed a critical value. In this sense, asymptotic mechanical hysteresis can appear <u>below</u> the endurance limit without signalizing

the onset of fatigue failure. This type of 'non-damaging' hysteresis is predicted both by our structural models as well as the general hysteresis theory. Experimentally, this behavior can be studied with scanning tunneling microscopy, acoustic emission, magnetomechanical response, and other effects that are sensitive to microstructural processes. Preliminary results have been obtained with several of these techniques. The next phase of the research will include a careful repetition and extension of our hysteresis experiments, a correlation with acoustic emissions and an integration of results obtained in complementary research efforts, conducted elsewhere, involving scanning tunneling microscopy and magneto-mechanical response.

5. REFERENCES

[1] Erber, T., Guralnick, S.A. and Latal, H.G., *A General Phenomenology of Hysteresis*, Annals of Physics 69, No. 1 161-192 (1972).

[2] Guralnick, S.A., *Incremental Collapse Under Conditions of Partial Unloading*, Publications, International Association for Bridge and Structural Engineering, Zurich Switzerland, 33, 64-84 (1973).

[3] Guralnick, S.A., *An Incremental Collapse Model for Metal Fatigue*, Publications, International Association for Bridge and Structural Engineering, Zurich Switzerland, 35, 83-99 (9175).

[4] Guralnick, S.A., Singh, S. and Erber, T., *Plastic Collapse, Shakedown Hysteresis*, J. Struct, Engng. ASCE, 110, 2103-2119 (1984).

[5] Guralnick, S.A., et al., *Plastic Collapse, Shakedown and Hysteresis of Multi-Story Steel Structures*, J. Struct. Engng., ASCE, 112, 2610-2627(1986).

[6] Gural[illegible], S.A., T., Soudan, O. and Stefanis, J., *Energy Method for Incremental Collapse Analysis of Framed Structures*, J. Struct. Engng. ASCE 114, 31-49 (1988).

[7] Erber, T. and Guralnick, S.A., *Hysteresis and Incremental Collapse: The Iterative Evolution of a Complex System*, Annals. Phys. 114, 25-53 (1988).

[8] Bernstein, B., Erber, T., Guralnick, S.A., *The Thermodynamics of Plastic Hinges With Damage*, Journal of Continuum Mechanics and Thermodynamics, Springer-Verlag, New York, N.Y., in press.

[9] Foppl, O., Iron and Steel Inst. 134, 393-423 (1936).

[10] Lazan, B.J., *Damping of Materials and Members in Structural Mechanics*, (Pergamon Press, 1988).

[11] Erber, T., Schweizer, B., and Sklar, A., Commun. Mathem. Phys. 20, 205-219 (1971).

[12] Weinstock, H., Erber, T., and Niesenoff, M., Phys. Rev. B31, No. 3, 1535-1553 (1985).

[13] Bridgman, P.W., Reviews of Modern Physics 22, No. 1, 56-63 (1950).

[14] Halford, G.R., *Stored Energy of Cold Work Changes Induced by Cyclic Deformation*, Ph.D. Dissertation, University of Illinois, unpublished, (1966).

[15] Halford, G.R., *The Energy Required for Fatigue*, Journal of Materials 1, No. 1, 3-18 (1966).

[16] Miner, M.A., *Cumulative Damage in Fatigue*, Journal of Applied Mechanics 12, No. 3, 159 (September 1945).

[17] Morrow, J., ASTM Special Technical Publication No. 378 (1965).

[18] Morrow, J., *Cyclic Plastic Strain Energy and Fatigue of Metals*, INSTRON application Series M-20.

[19] Palmgren, A., *The Endurance of Ball Bearings* (in German), Z. Wer. Deut., Ing. 68, 339, (April 1924).

[20] French, H.J., *Fatigue and the Hardening of Steels, Transactions*, A.S.S.T., (October, 1933), pp. 899-946.

[21] Coffin, L.F., Jr., *"Low Cycle Fatigue: A Review"*, Applied Materials Research, 1(3), 129-141, October 1962.

[22] Manson, S.S., *"Interpretive Report on Cumulative Fatigue Damage in the Low Cycle Range"*, Welding Journal, 43(8), Research Supplement, 3445-3525, 1964.

[23] Basquin, O.H., *"The Exponential Law of Endurance Tests"*, American Society of Testing Materials, Proc., Vol. 10, (1910), pp. 625-630.

TABLE 1

Chemical Properties Of
Rimmed ASTM 1018 Steel

ELEMENT	PERCENT BY WEIGHT
CARBON	0.16
MANGANESE	0.75
PHOSPHOROUS	0.012
SULFUR	0.016
SILICON	0.04
NICKEL	0.04
CHROMIUM	0.04
COPPER	0.06
MOLYBDENUM	0.02

TABLE 2
UNIAXIAL TENSILE PROPERTIES (MONOTONIC LOADING TO FAILURE)
(AISI 1018 Unannealed Steel)

SPECIMEN NUMBER	DIAMETER (In.)	GAGE LENGTH (In.)	YIELD STRENGTH* (PSI)	ULTIMATE STRENGTH (PSI)	ELONGATION (%)	REDUCTION IN AREA (%)
AX121	0.505	2.000	70,150	77,090	18.05	61.83
AX122	0.506	2.000	69,620	77,280	18.40	61.74
AX221	0.506	2.000	71,610	78,270	17.95	61.25
AX222	0.506	2.000	72,360	78,570	18.65	61.49
AX321	0.506	2.000	72,110	79,370	17.20	58.75
AX322	0.506	2.000	71,610	79,370	17.25	58.49
AX421	0.506	2.000	67,880	74,490	19.10	61.98
AX422	0.506	2.000	68,130	74,390	18.70	62.47
AX521	0.506	2.000	72,110	79,170	18.40	61.00
AX522	0.506	2.000	72,110	79,170	18.30	61.49
		AVERAGE	70,769	77,717	18.20	61.05

*Yield Strength is obtained at 0.2% offset.

TABLE 3

TEST TYPE: Strain control, virgin specimens tested to failure.

SPECIMEN NAME	STRAIN AMPLITUDE (IN/IN)	CYCLES TO FAILURE	CUMULATIVE HYSTERESIS LOSS	AVERAGE HYSTERESIS LOSS
FTG124	0.0035	17,843	4,010.9	0.2248
FTG125	0.0045	6,537	2,400.68	0.3668
FTG127	0.006	2,472	1,502.44	0.6079
FTG128	0.015	118	293.846	2.5041
FTG129	0.008	532	552.329	1.0437
FTG132	0.003	24,854	3,661.688	0.1473
FTG222	0.015	101	252.347	2.5182
FTG223	0.008	754	756.005	1.0028
FTG224	0.006	2,485	1,469.279	0.5886
FTG225	0.003	30,276	4,600.180	0.1519
FTG226	0.0045	3,949	1,480.548	0.3750
FTG233	0.0035	10,821	2,301.857	0.2126
FTG323	0.0045	4,560	1,412.978	0.3105

TABLE 4

TEST TYPE: Strain controlled, varying number of cycles. Samples with the letter A appended to the sample name are virgin specimens, while other letters indicate the same specimens retested at different strain levels.

SPECIMEN NAME	STRAIN AMPLITUDE	CYCLES TESTED	AVERAGE HYSTERESIS LOSS
FTG227A	0.0022	360	0.0626
FTG227B	0.0035	360	0.2250
FTG227C	0.0045	360	0.3595
FTG228A	0.0022	360	0.0684
FTG228B	0.0025	360	0.1039
FTG228C	0.003	360	0.1423
FTG228D	0.0035	360	0.2060
FTG228E	0.003	360	0.1457
FTG228F	0.0025	360	0.0970
FTG228G	0.0022	360	0.0710
FTG229A	0.0015	360	0.0059
FTG229B	0.0017	360	0.0197
FTG229D	0.0019	360	0.0408
FTG229E	0.0035	200	0.2194
FTG229F	0.004	200	0.2874
FTG229G	0.0045	200	0.3602
FTG229H	0.005	200	0.4357
FTG229I	0.0045	200	0.3566
FTG229J	0.004	200	0.2839
FTG229K	0.0035	200	0.2156

TABLE 4 (CONTINUED)

SPECIMEN NAME	STRAIN AMPLITUDE	CYCLES TESTED	AVERAGE HYSTERESIS LOSS
FTG230A	0.0022	200	0.0551
FTG230B	0.0025	200	0.0941
FTG230C	0.0028	200	0.1290
FTG230D	0.0033	200	0.1888
FTG230E	0.0040	200	0.2805
FTG230F	0.0055	100	0.5115
FTG230G	0.0065	50	0.6789
FTG230H	0.0100	50	1.3673
FTG230I	0.0065	50	0.6754
FTG230J	0.0055	100	0.5049
FTG230K	0.0040	200	0.2783
FTG230L	0.0033	200	0.1866
FTG230M	0.0028	200	0.1304
FTG230N	0.0025	200	0.0999
FTG230O	0.0022	200	0.0736

TABLE 4 (CONTINUED)

SPECIMEN NAME	STRAIN AMPLITUDE	CYCLES TESTED	AVERAGE HYSTERESIS LOSS
FTG231A	0.0022	400	0.0708
FTG231B	0.0021	40	0.0649
FTG231C	0.0020	40	0.0571
FTG231D	0.0019	40	0.0493
FTG231E	0.0018	40	0.0425
FTG231F	0.0017	40	0.0357
FTG231G	0.0016	40	0.0303
FTG231H	0.0015	40	0.0236
FTG231I	0.0014	40	0.0194
FTG231J	0.0013	40	0.0137
FTG231K	0.0012	40	0.0090
FTG231L	0.0011	40	0.0049
FTG231M	0.0010	40	0.0033
FTG231N	0.0011	40	0.0050
FTG231O	0.0012	40	0.0075
FTG231P	0.0013	40	0.0108
FTG231Q	0.0014	40	0.0149
FTG231R	0.0015	40	0.0194
FTG231S	0.0016	40	0.0243
FTG231T	0.0017	40	0.0306
FTG231U	0.0018	40	0.0366
FTG231V	0.0019	40	0.0432
FTG231W	0.0020	40	0.0499
FTG231X	0.0021	40	0.0591

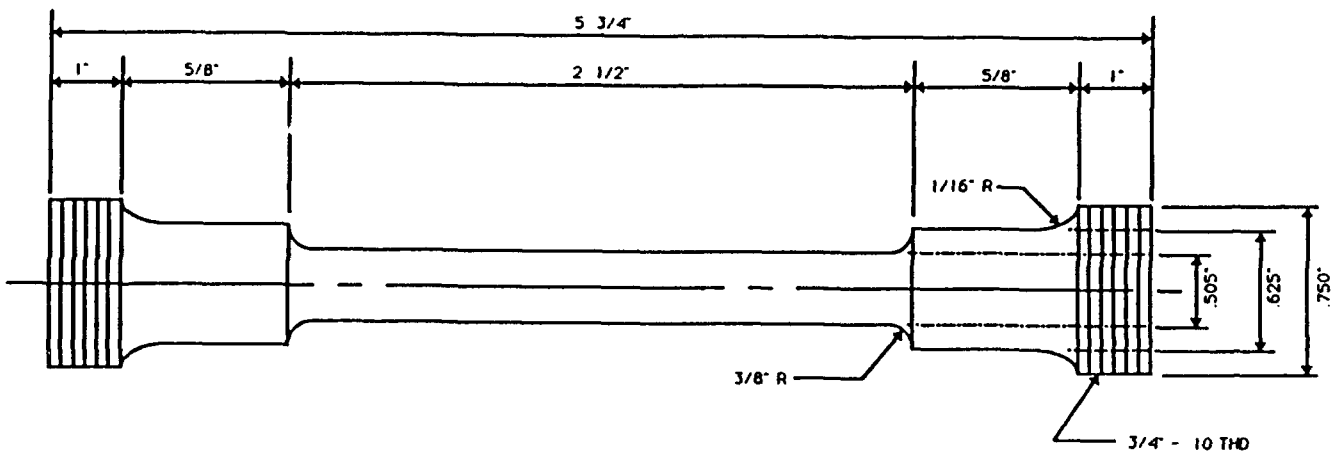

FIG. A ASTM TYPE 2 AXIAL LOAD TENSION SPECIMEN
(3/4" DIAMETER ROD STOCK)

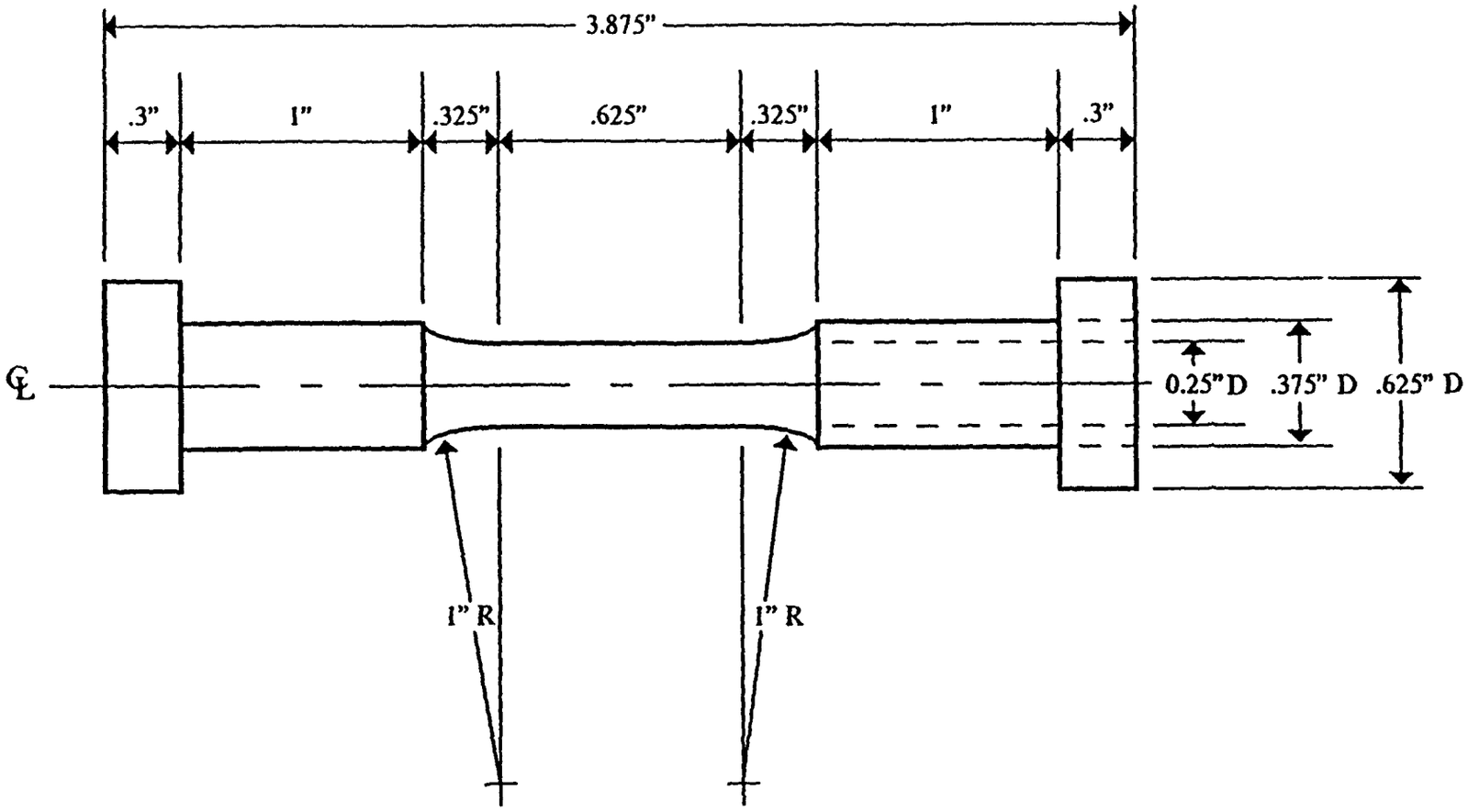

Fig. B Axial Load Fatigue Specimen
(3/4" Diam. Rd. Stock)

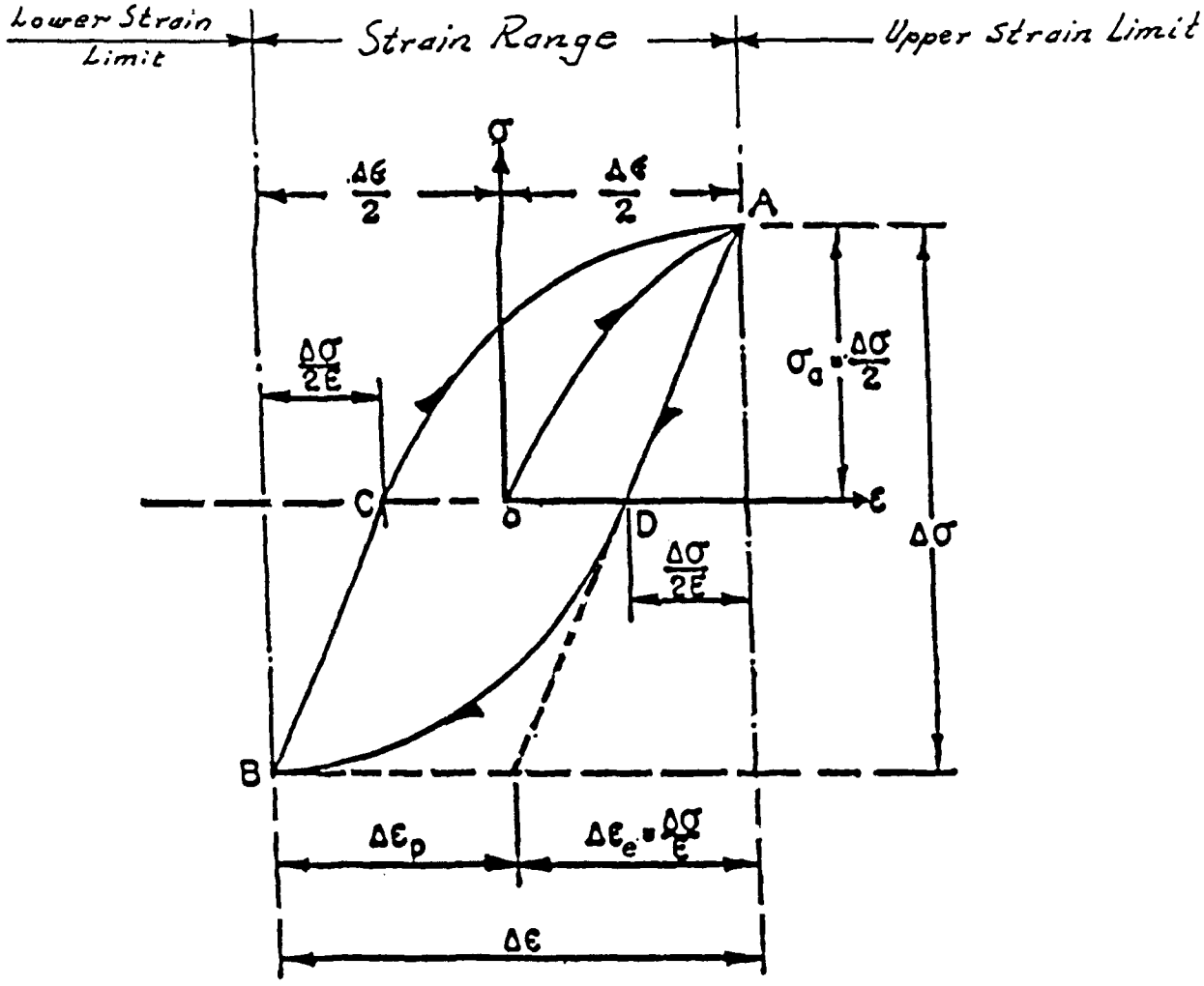

Fig. 1 Typical Stress-Strain Loop for Constant Strain Range Cycling

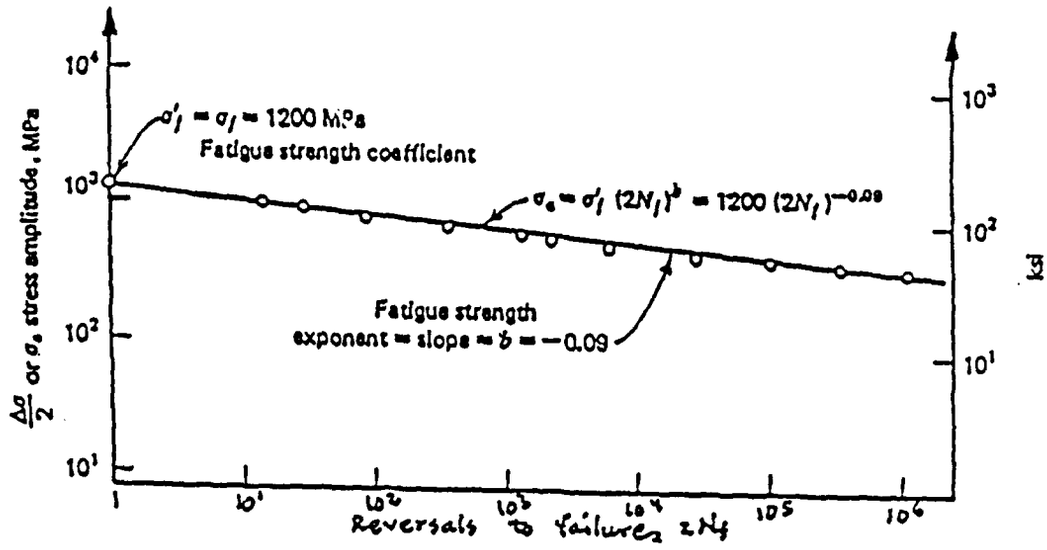

Fig. 2 Fatigue Strength Properties

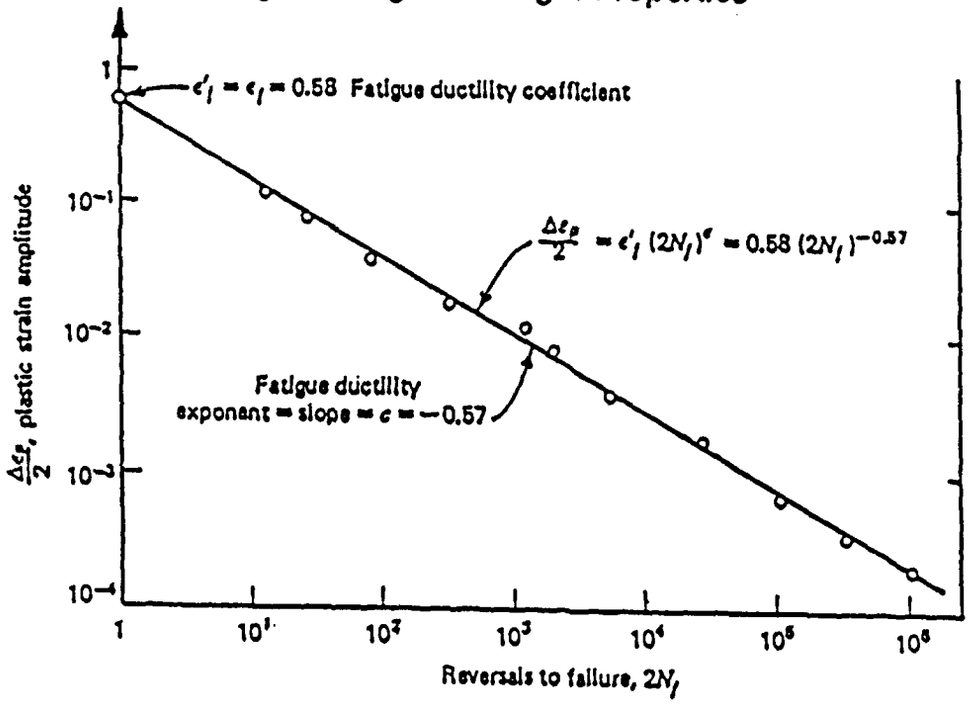

Fig. 3 Fatigue Ductility Properties

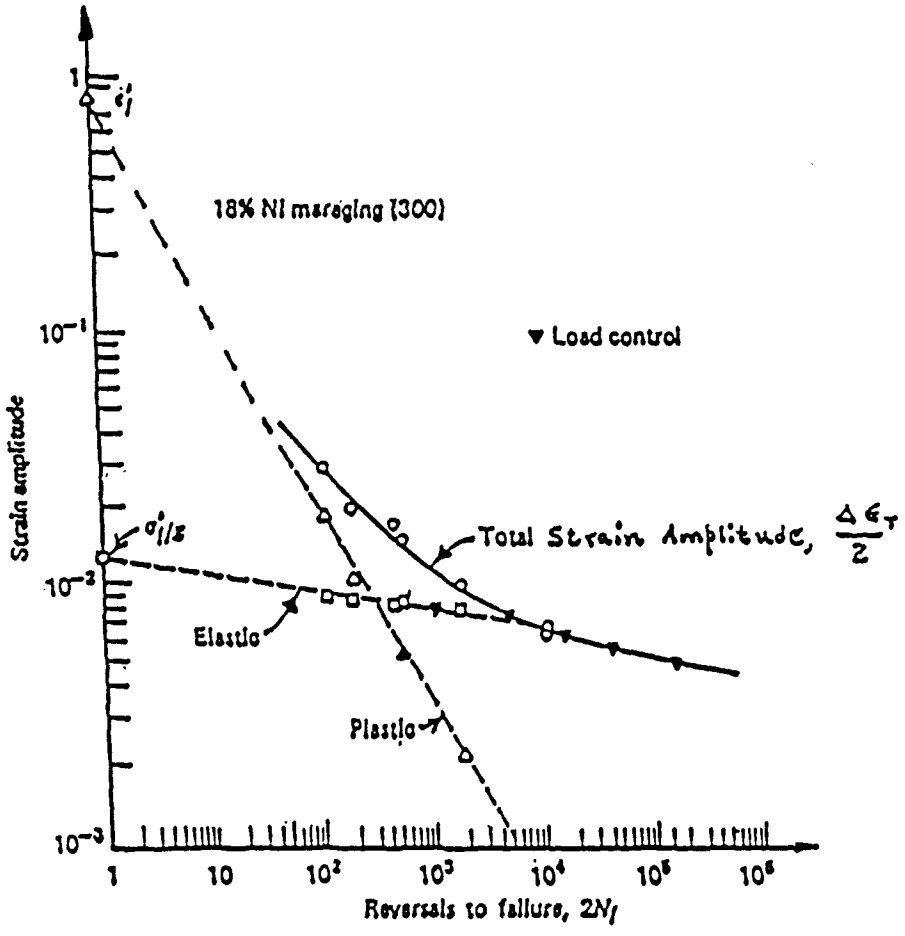

Fig. 4 Typical Strain Amplitude vs Life Data

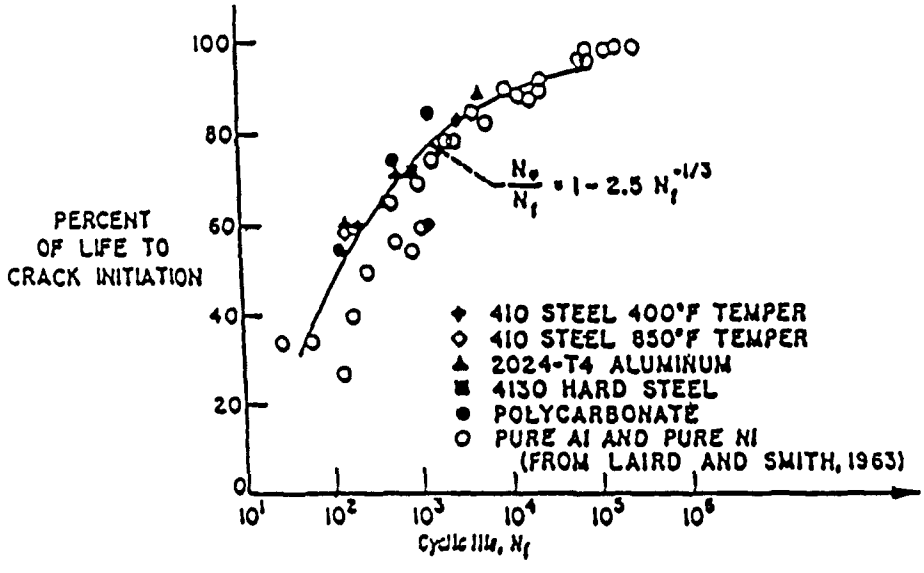

Fig. 5 Percent of Life to Crack Initiation vs Life Data for Several Materials

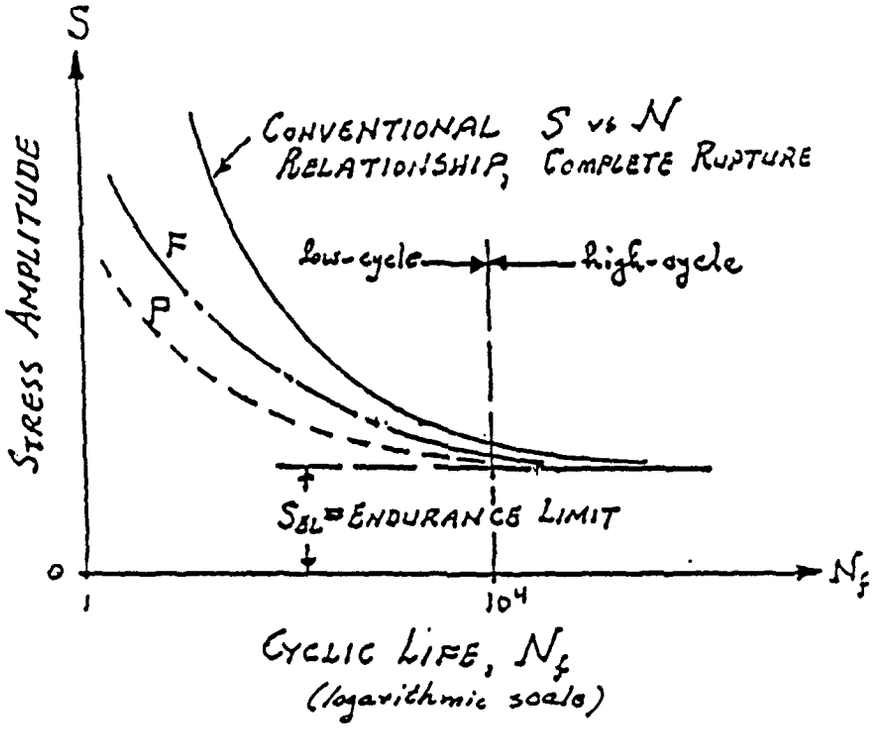

Fig. 6 The Evolution of the S-N Curve From Stages of Microplasticity and Crack Initiation

Fig.7 *S-N* Curves Typical for Medium-Strength Steels *

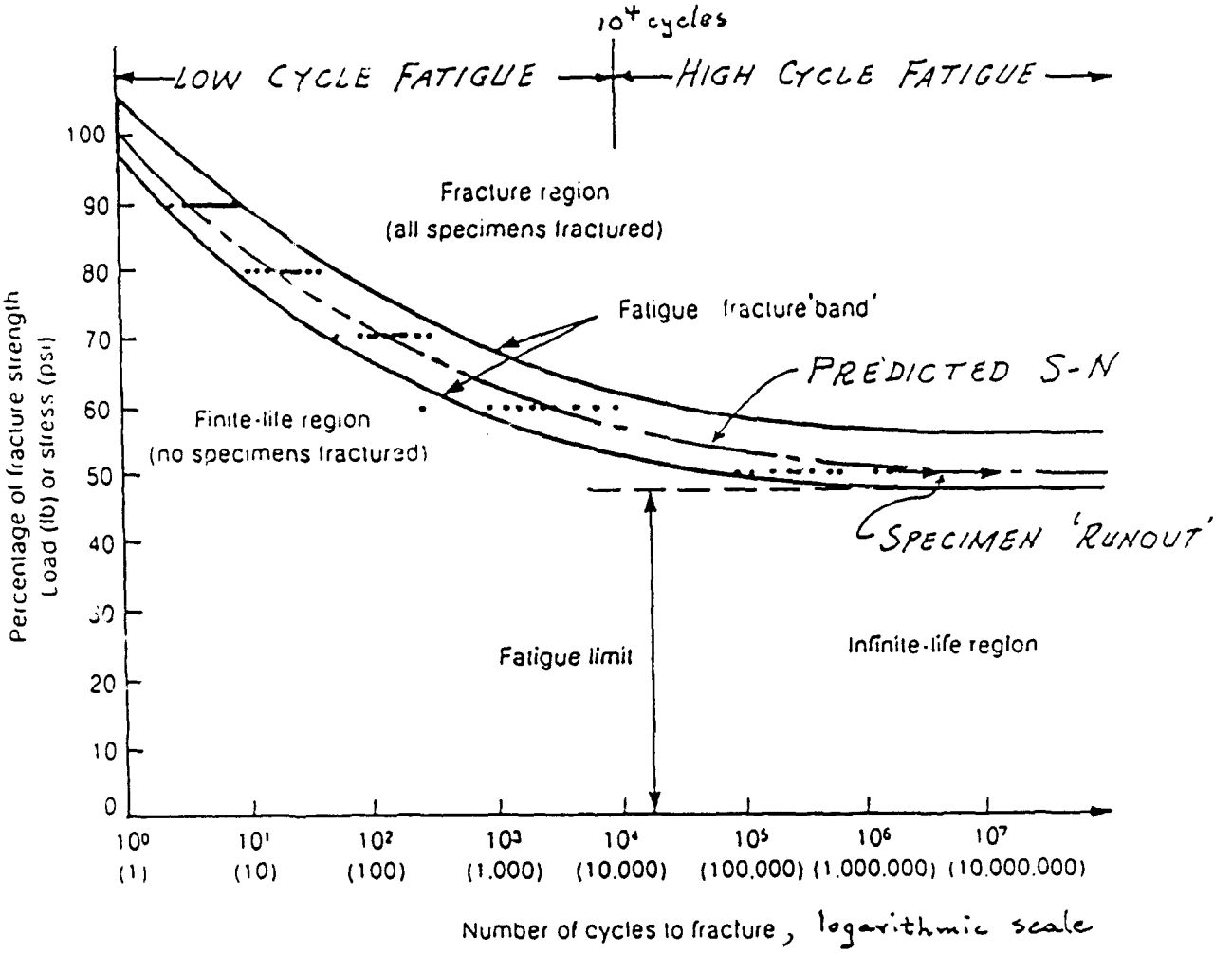

* From Boyer, H.E., "Atlas of Fatigue Curves", American Society for Metals, May 1986.

Fig 8A. CYCLIC STRESS - STRAIN AND MONOTONIC STRESS - STRAIN

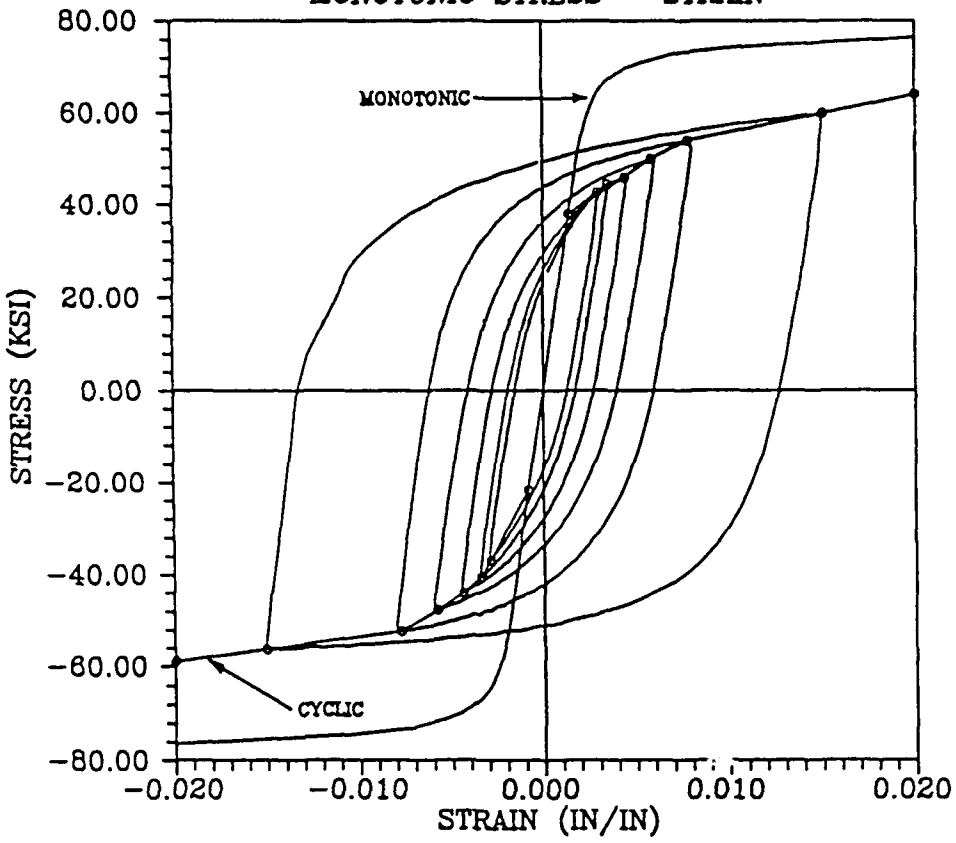

Fig. 8b CYCLIC STRESS - STRAIN AND MONOTONIC STRESS - STRAIN

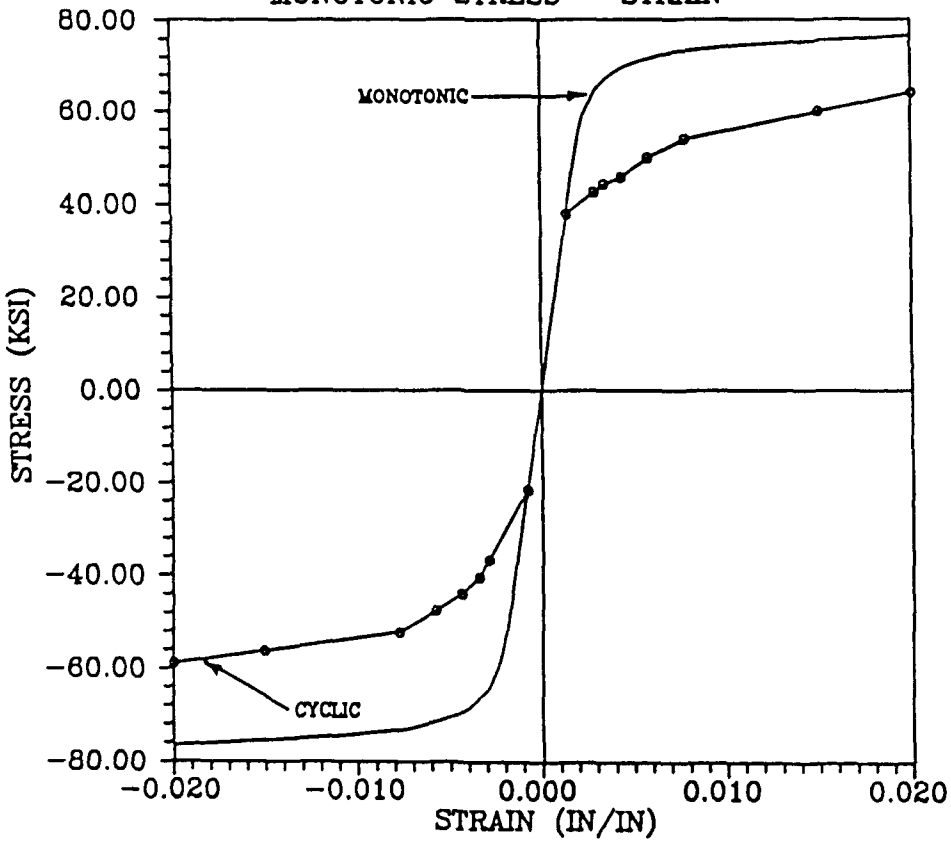

Fig. 9 FATIGUE STRENGTH PROPERTIES
$\Delta\sigma/2$ VS $2N_f$

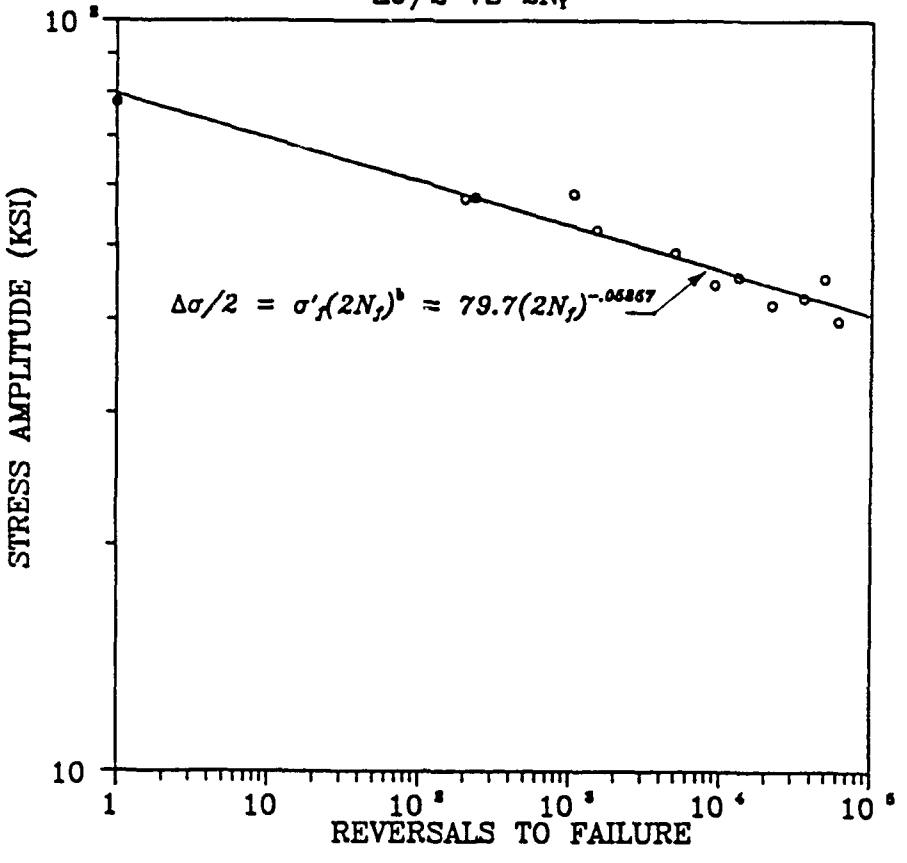

Fig. 10 FATIGUE DUCTILITY PROPERTIES
$\Delta\varepsilon_p/2$ VS $2N_f$

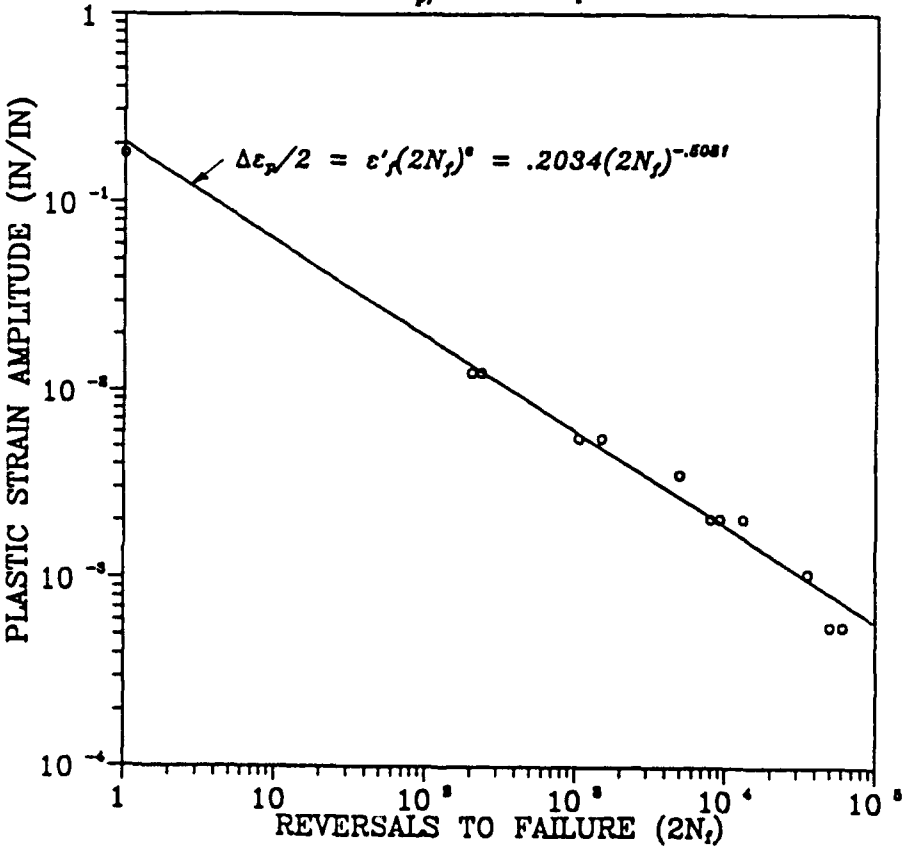

Fig. 11 STRAIN AMPLITUDE VS REVERSALS TO FAILURE

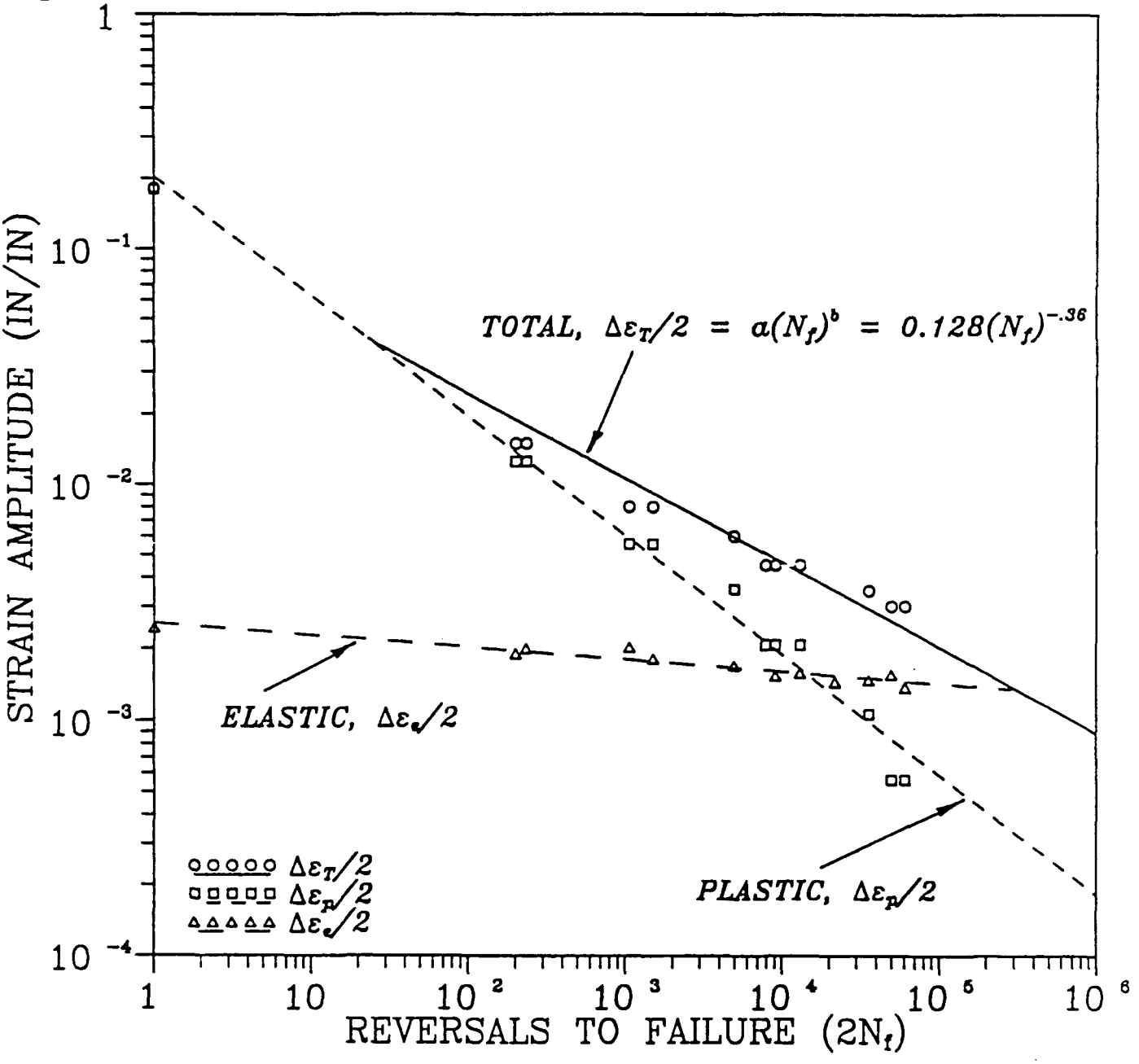

Fig. 12 TYPICAL 'STAIRCASE' LOADING PROGRAM

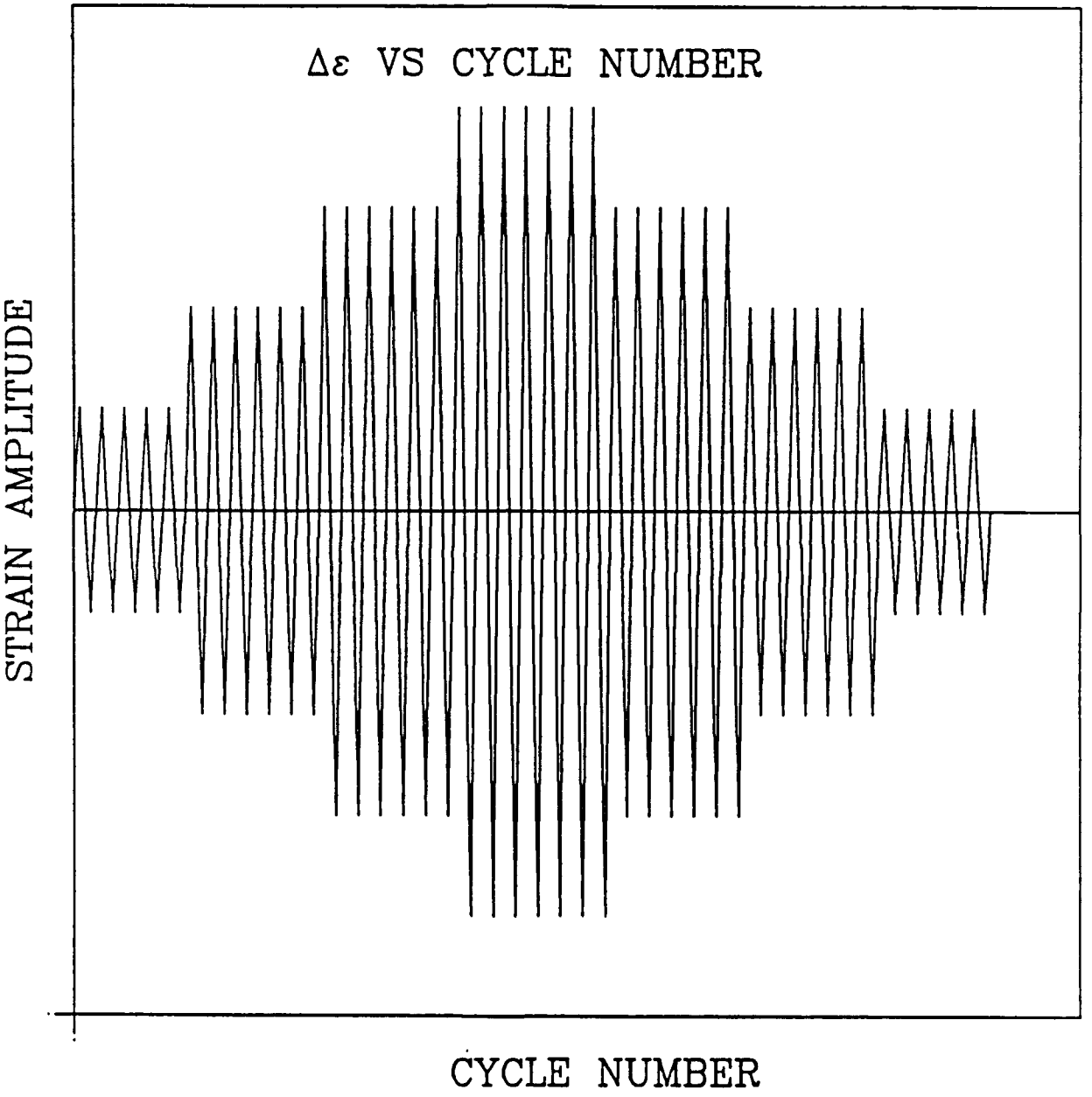

Fig. 13a HYSTERESIS LOSS PER CYCLE VS CYCLES
ΔU_i VS N_f
$\Delta\varepsilon_T/2 = 0.0045$

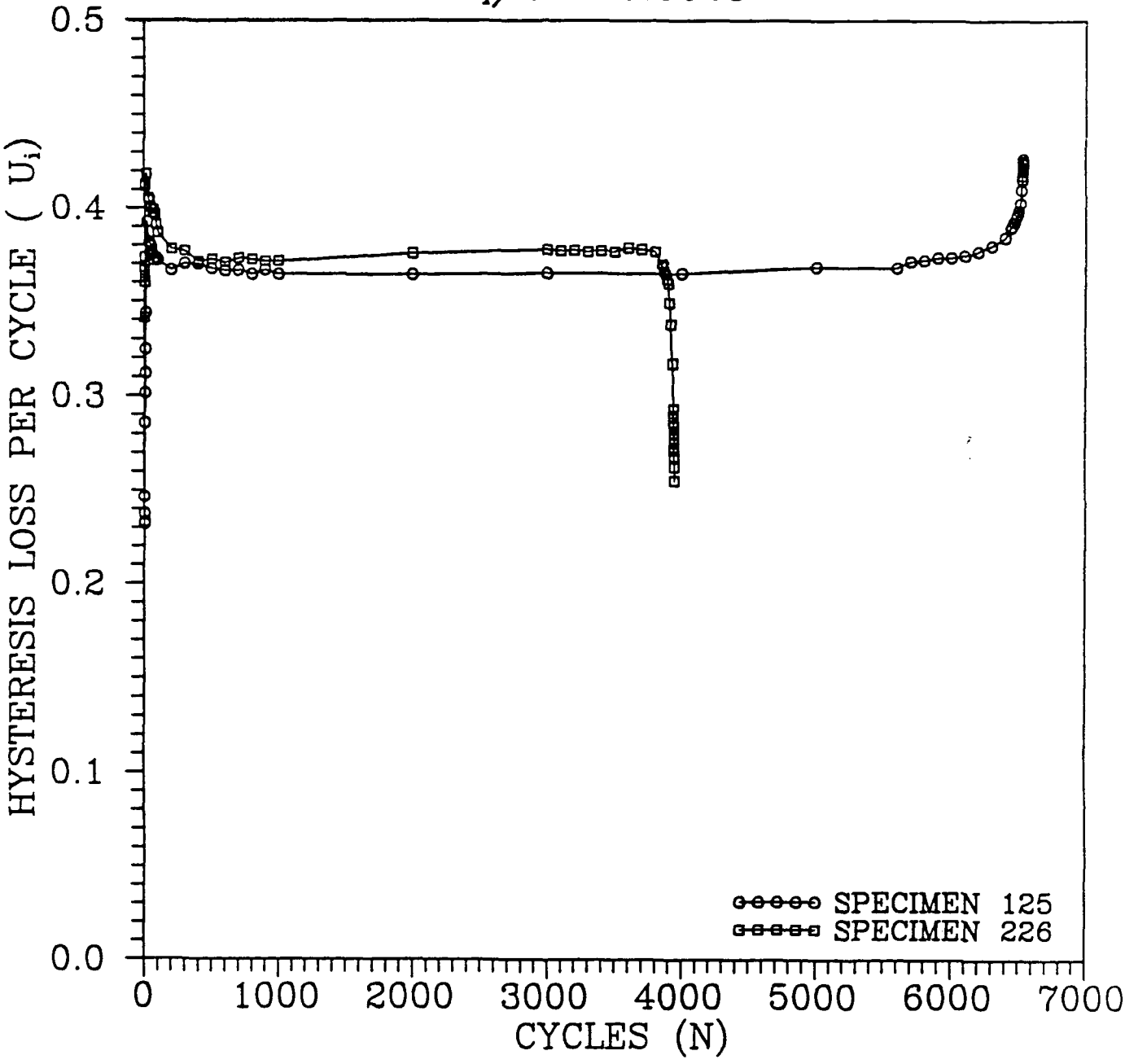

Fig. 13b HYSTERESIS LOSS PER CYCLE VS CYCLES
ΔU_i VS N_f
$\Delta\varepsilon_T/2 = 0.008$

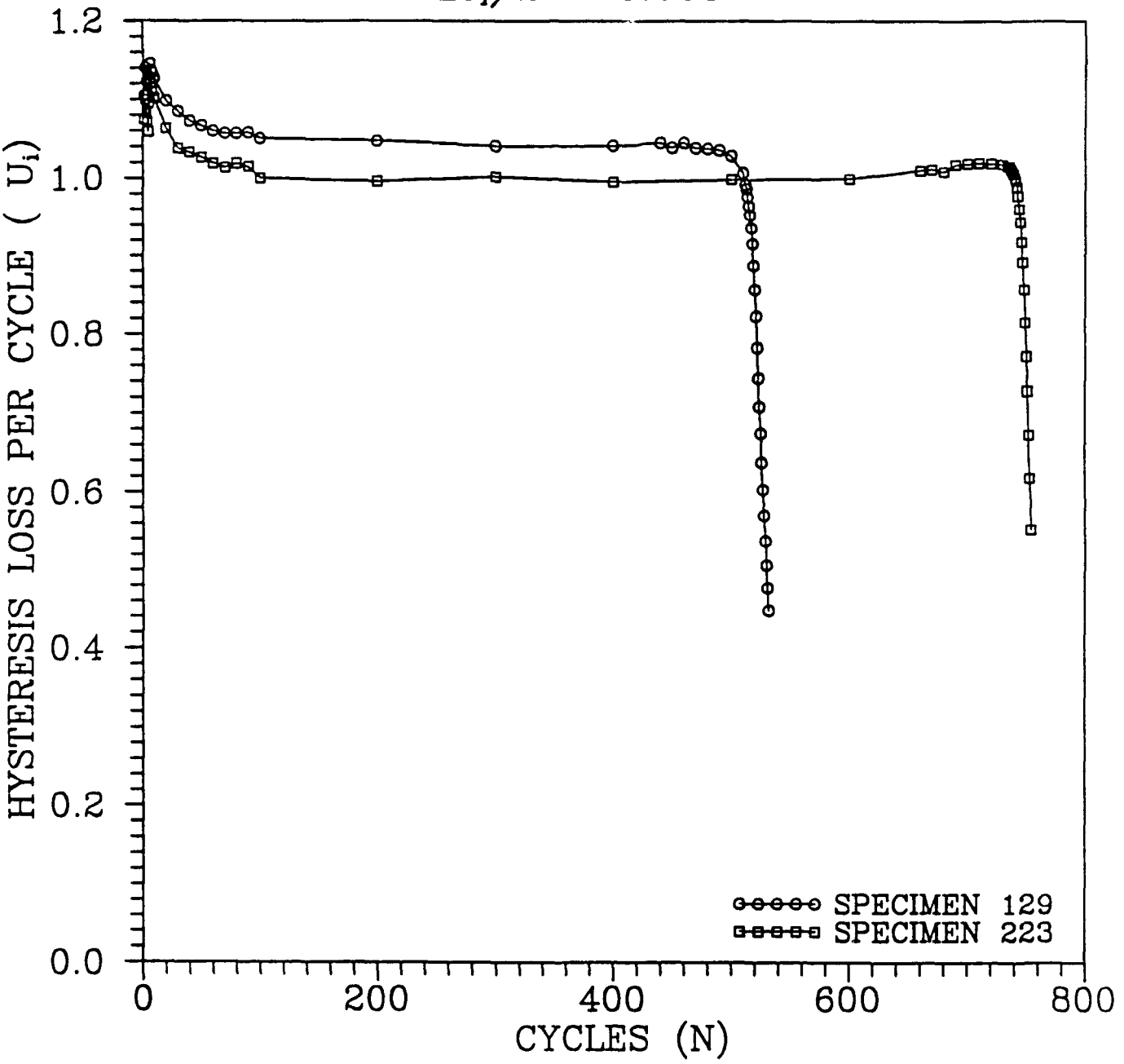

Fig. 13c HYSTERESIS LOSS PER CYCLE VS CYCLES
ΔU_i VS N_f
$\Delta\varepsilon_T/2 = 0.015$

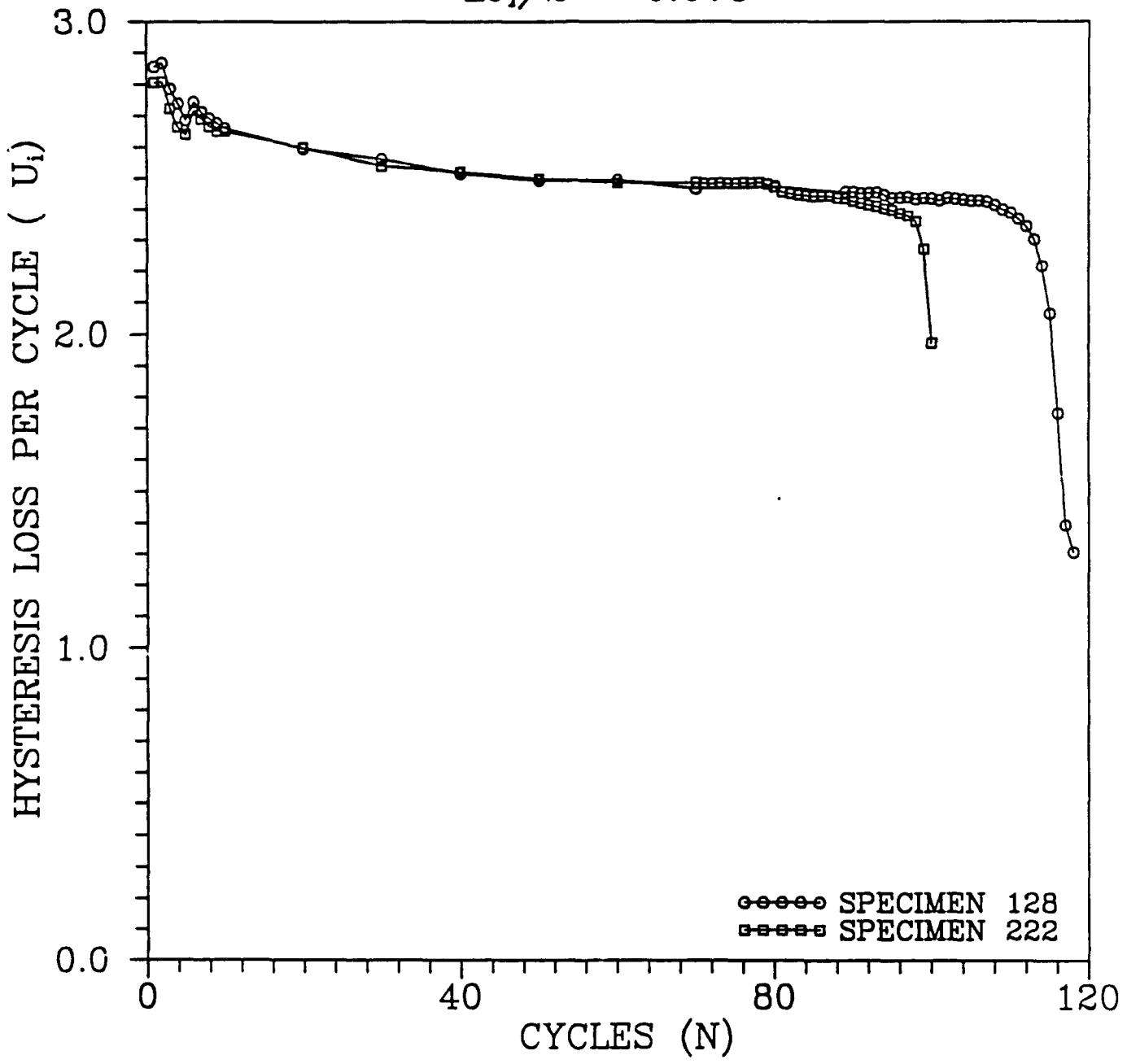

Fig. 14a CUMULATIVE HYSTERESIS LOSS VS CYCLES
$\Sigma(\Delta U_i)$ VS N

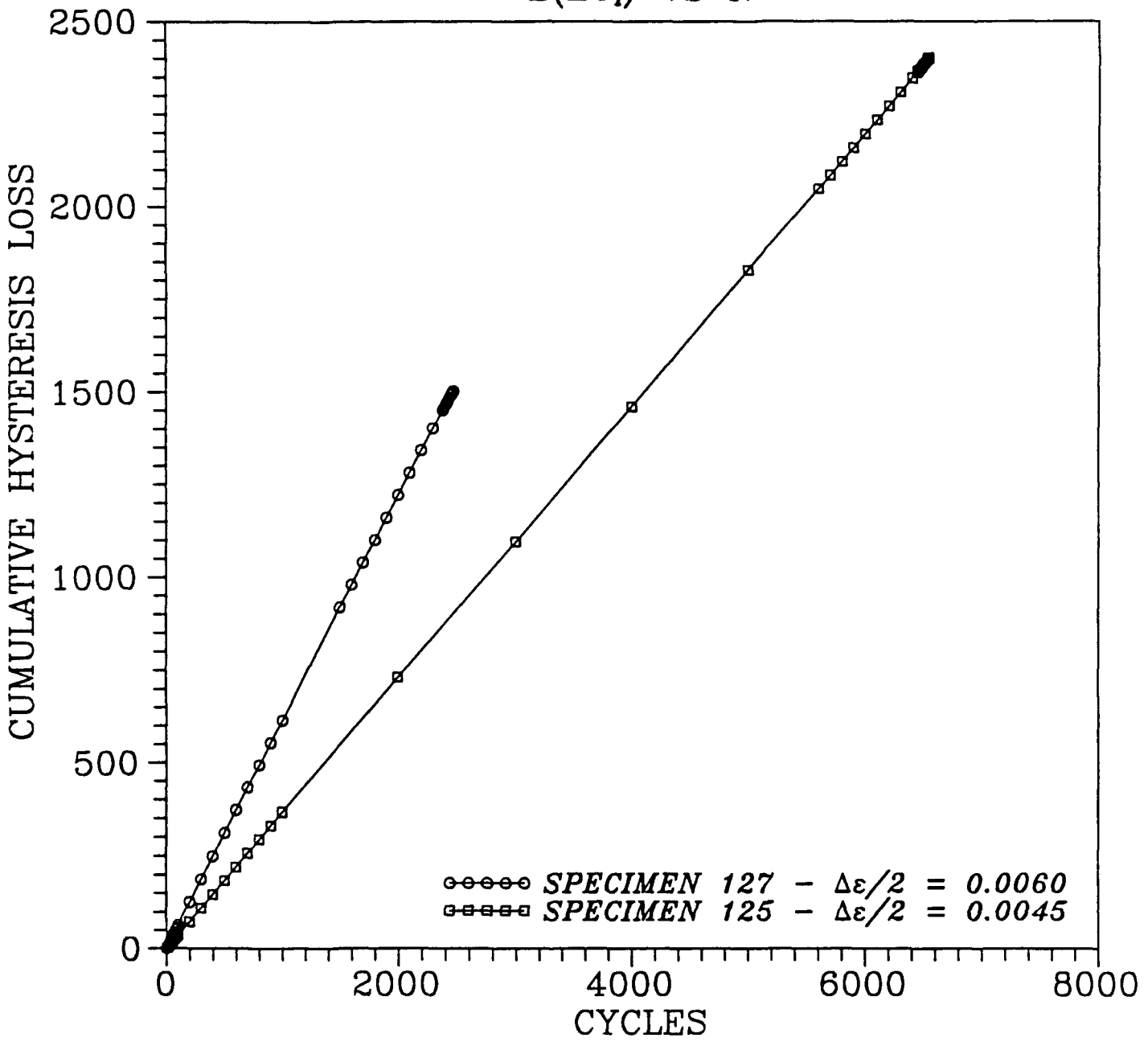

Fig. 14b CUMULATIVE HYSTERESIS LOSS VS CYCLES
$\Sigma(\Delta U_i)$ VS N

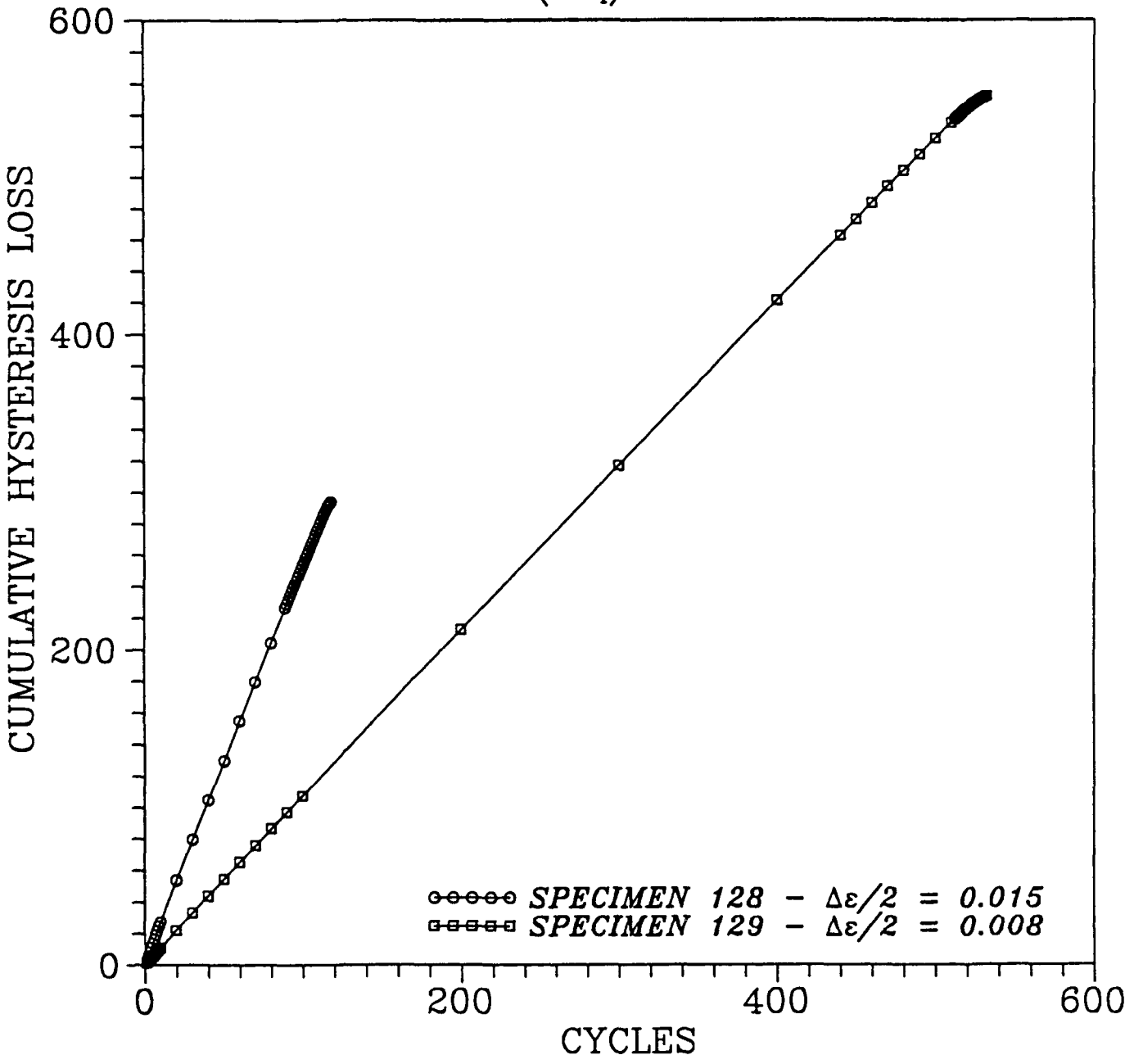

Fig. 15 CUMULATIVE HYSTERESIS LOSS AT FAILURE VS CYCLES TO FAILURE
U_f VS N_f

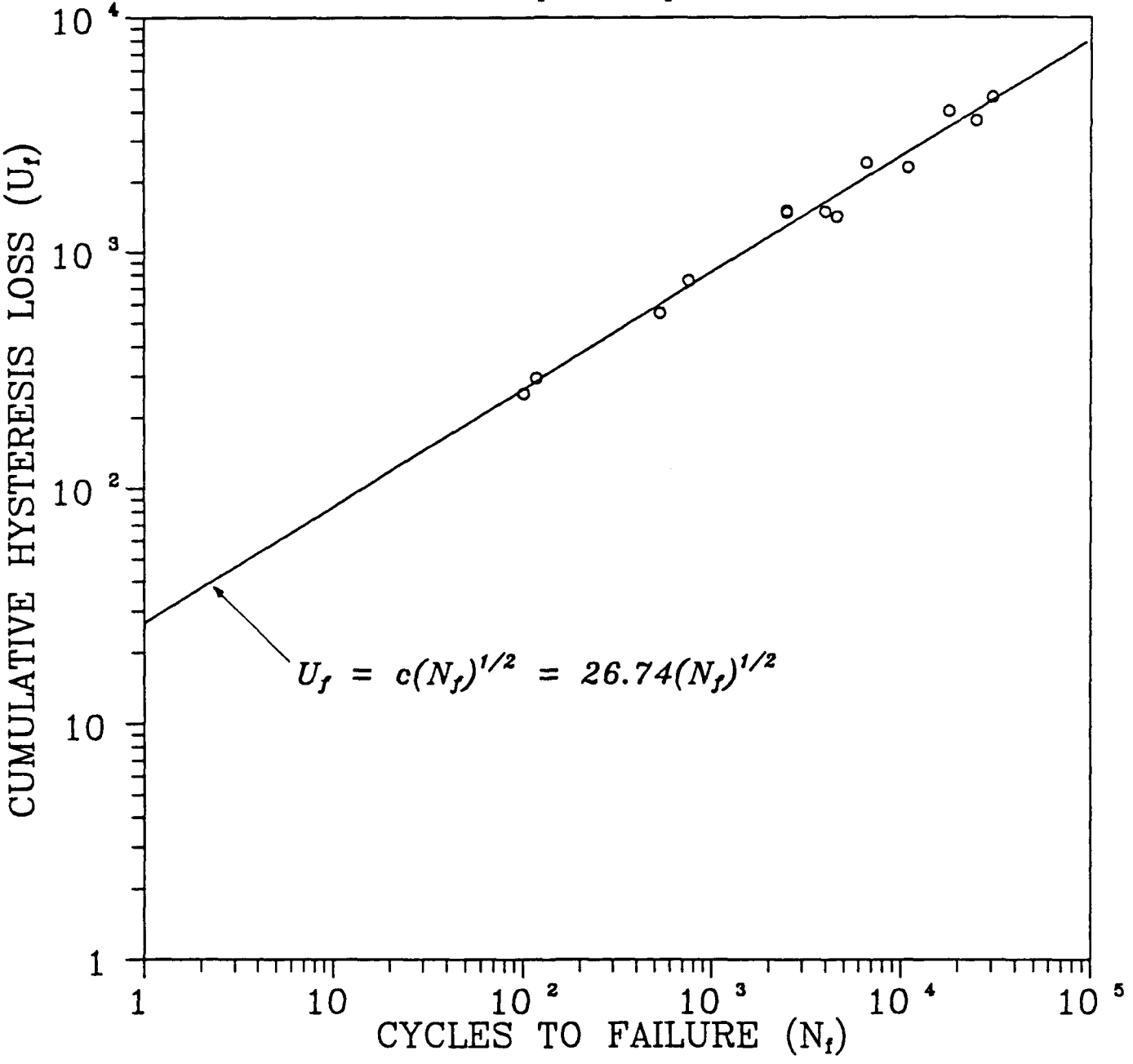

Fig. 16a AVERAGE HYSTERESIS LOSS VS STRAIN AMPLITUDE

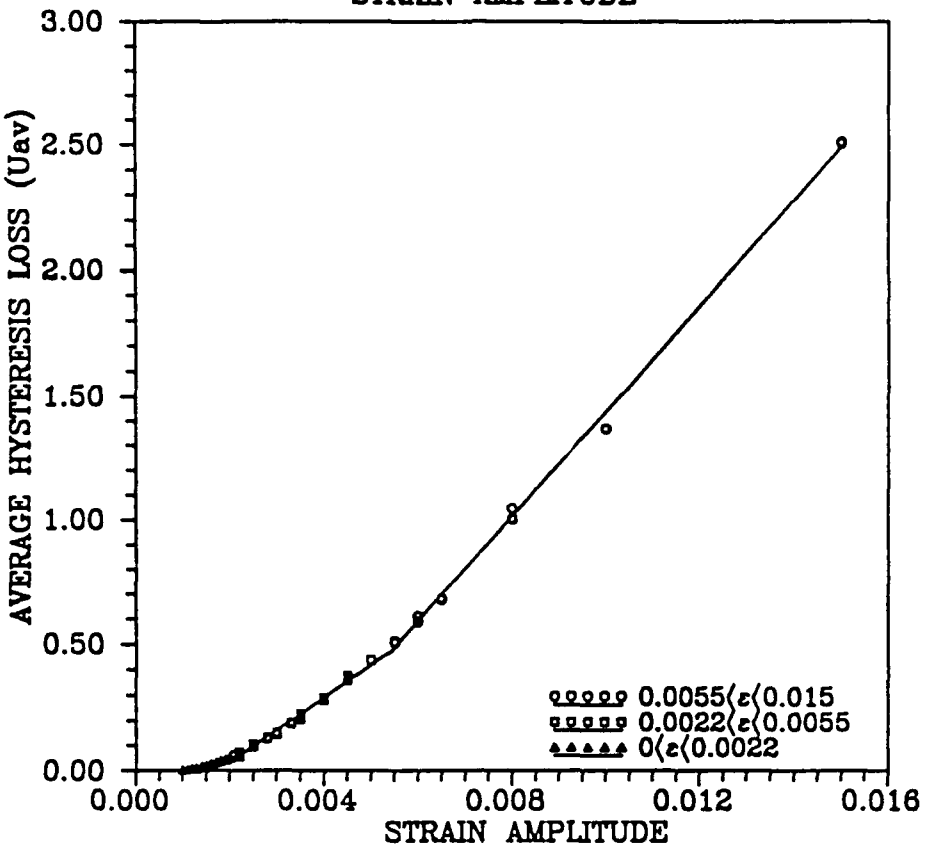

Fig 16b AVERAGE HYSTERESIS LOSS VS STRAIN AMPLITUDE, EXPANDED VIEW

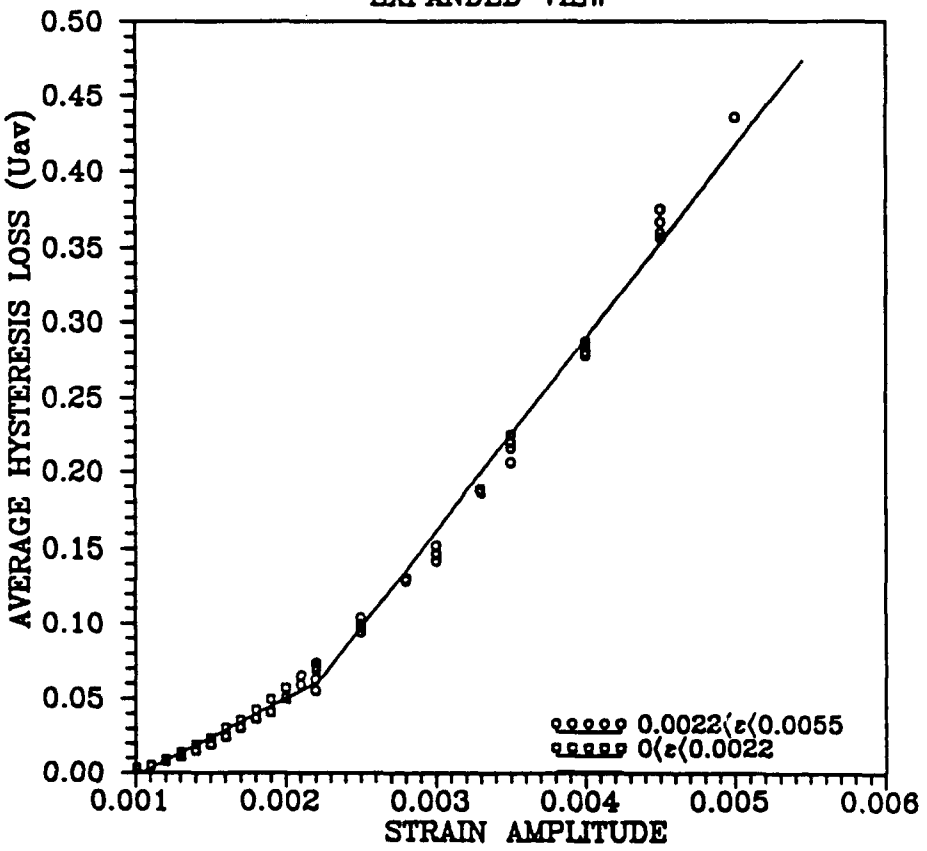

Fig. 17 CUMULATIVE HYSTERESIS LOSS AS A FUNCTION OF STRAIN AMPLITUDE AND CYCLES TO FAILURE
$U_f = U_f(N_f, \Delta\varepsilon_T/2)$

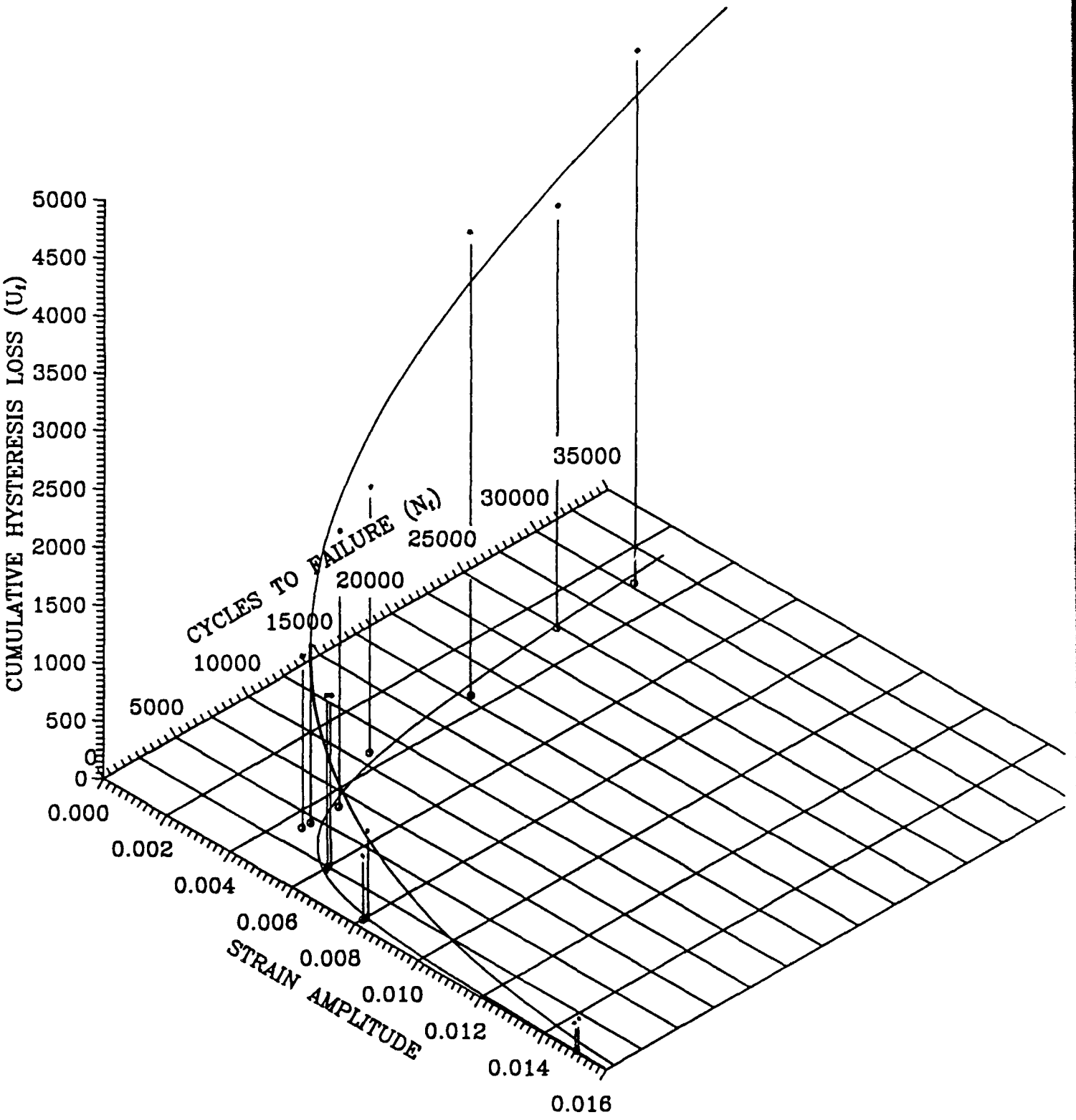

Fig. 1C CONNECTION BETWEEN CUMULATIVE HYSTERESIS LOSS AND STRAIN AMPLITUDE AT FAILURE IN FATIGUE